Near Surface Geophysics

Comparison of Stabilizer Functions for Surface NMR Inversions

Journal:	*Near Surface Geophysics*
Manuscript ID	nsg-2016-1460.R2
Manuscript Type:	Original Article
Date Submitted by the Author:	n/a
Complete List of Authors:	Grombacher, Denys; Aarhus Universitet, Geoscience Fiandaca, Gianluca; Aarhus University, Geoscience Behroozmand, AhmadA.; Stanford University, Geophysics Auken, Esben; Aarhus University, Department of Geoscience
Keywords:	Surface nuclear magnetic resonance, Groundwater, Inversion

Comparison of Stabilizer Functions for Surface NMR Inversions

Denys Grombacher[1], Gianluca Fiandaca[1], Ahmad A. Behroozmand[2], and Esben Auken[1]

[1]Department of Geoscience, Aarhus University, [2]Department of Geophysics, Stanford University

Corresponding author email : denys.grombacher@geo.au.dk

List of keywords : Surface nuclear magnetic resonance, groundwater, inversion

ABSTRACT

Surface nuclear magnetic resonance (NMR) is a geophysical technique providing non-invasive aquifer characterization. Two approaches are commonly used to invert surface NMR data: 1) inversions involving many depth layers of fixed thickness, and 2) few layer inversions without predetermined layer thicknesses. The advantage of the many layer approach is that it requires little a priori knowledge. However, the many layer inversion is extremely ill-posed and regularization must be used to produce a reliable result. For optimal performance the selected regularization scheme must reflect all available a priori information. The standard regularization scheme for many layer surface NMR inversions employs a L_2 smoothness stabilizer, which results in subsurface models with smoothly varying parameters. Such a stabilizer struggles to reproduce sharp contrasts in subsurface properties, like those present in a layered subsurface (a common near-surface hydrogeological environment). To investigate if alternative stabilizers can be used to improve the performance of the many layer inversion in layered environments the performance of the standard smoothness stabilizer is compared against two alternative stabilizers: 1) a stabilizer employing the L_1 norm and 2) a minimum gradient support stabilizer. Synthetic results are presented to compare the performance of the many layer inversion for the different stabilizer functions. The minimum gradient support stabilizer is observed to improve performance of the many layer inversion for a layered subsurface, being able to reproduce both smooth and sharp vertical variations of the model parameters. Implementation of the alternative stabilizers into existing surface NMR inversion software is straightforward and requires little modification to existing codes.

INTRODUCTION

Surface nuclear magnetic resonance (NMR) is a non-invasive geophysical technique providing insight into aquifer properties. The measurement involves pulsing strong oscillatory currents in a surface coil in order to generate a measureable NMR signal at depth that originates from the immersion of hydrogen nuclei in the Earth's magnetic field (Schirov et al., 1991; Hertrich, 2008). To gain insight into the spatial variability of aquifer properties, the amplitude of the pulsed current is varied to manipulate the spatial origin of the measured signal. This procedure is typically referred to as a sounding, where weak and strong currents produce signals from shallow and greater depths, respectively. The end product is a data set containing NMR signals of differing spatial origins (although many signals have overlapping spatial origins). An inversion framework is used to estimate the underlying spatial distribution of aquifer properties consistent with the observed data. This involves minimizing an objective function that is used to penalize undesirable model characteristics, such as penalizing models that do not closely reproduce the observed data.

Several inversion schemes are commonly employed in surface NMR, such as the time step inversion (Legchenko and Valla, 2002), the QT-inversion that inverts the entire data cube simultaneously (Müller-Petke and Yaramanci, 2010), joint-inversion schemes coupling NMR and time-domain electromagnetic (TEM) data (Behroozmand et al., 2012) or NMR and electrical resistivity (Günther et al., (2012) data, and frequency-domain inversions (Irons and Li, 2014). In each case, the inversion result is a model of the subsurface aquifer properties (such as depth profiles of the water content and relaxation times that describe the duration of the NMR signal). For the purposes of this discussion we group surface NMR inversions into two categories: 1) inversions that use model domains consisting of many depth layers of fixed depths and thickness (referred to as many layer inversions), and 2) inversions involving relatively small model domains with few depth layers, where the inversion determines the thickness of each layer (referred to as few layer inversions). Each of the previously mentioned surface NMR inversion schemes may be implemented using either a many layer or few layer model domain.

In many layer inversions the number of model parameters is generally quite large (when compared with few layer inversions) and a regularization term must be included in the objective function to stabilize the ill-posed inversion (Tikhonov and Arsenin, 1977). The model that minimizes the objective function thus balances satisfactory data fit with the magnitude of the regularization term, which is controlled by the stabilizer function and the characteristics of the model. For optimal results the selected stabilizer function should: 1) return small values for the regularization term when the model exhibits features consistent with a priori knowledge about the site, and 2) return large values for models with characteristics inconsistent with a priori information about the site. The standard stabilizer in surface NMR is the L_2 smoothness stabilizer, which penalizes the square of the variation between neighboring model parameters. For a 1D depth sounding (the standard surface NMR experiment), this results in models that vary smoothly with depth. A limitation of such an approach is that the inversion struggles to reproduce sharp variations in water contents and relaxation times that may be present at the interface between lithologic layers of contrasting properties. To address this concern, an alternative stabilizer may be employed, such as the minimum support (Last and Kubik, 1983), minimum gradient support (Portniaguine and Zhdanov, 1999), or stabilizers based on L_1 norms (e.g. Ellis and Oldenburg, 1994; Loke et al., 2003). Mohnke and Yaramanci (2002) demonstrated the use of an L_1 stabilizer in surface NMR, but to our knowledge the smoothness stabilizer remains the standard in surface NMR.

For few layer inversions, a predetermined amount of layers is set and the inverted parameters are layer thicknesses, water contents, and relaxation times (Guillen and Legchenko, 2002; Mohnke and Yaramanci, 2002; Weichman et al., 2002). Due to the reduced number of model parameters (compared to the many layer inversion) no regularization term is included in the objective function. As a result, few layer inversions are well suited to produce models with sharp contrasts in water content and relaxation times between neighboring layers. An advantage of few layer inversions is that uncertainty in the estimated profiles can be readily quantified using Bayesian approaches such as Markov Chain Monte Carlo (Guillen and Legchenko, 2002; Weichman et al., 2002) or simulated annealing (Mohnke and Yaramanci, 2002). A limitation of few layer inversions is that they struggle to reproduce smoothly varying subsurface parameters and can exhibit strong sensitivity to the initial starting model (i.e. the a priori specification of the number of layers and layer properties).

In practice selection of a many layer versus few layer inversion scheme in surface NMR typically depends on how much a priori information is available. Many layer inversions are preferable given no a priori information, while few layer inversions may be preferable if a known number of layers are present. Few layer inversions are also commonly used if a well stratified subsurface is expected, given that many layer inversions typically result in models with smoothly varying subsurface parameters. However, this is not a result of the many layer inversion scheme directly, but rather a consequence that it generally employs a smoothness stabilizer. To balance the advantages of both inversion strategies for layered subsurfaces (i.e. the ability to reproduce sharp variations in model parameters without requiring extensive a priori information) the performance of several stabilizer functions is compared against the smoothness stabilizer; a minimum gradient support (MGS) stabilizer and a stabilizer employing an L_1 norm are investigated. Selecting alternative stabilizers does not require significant changes to existing inversions schemes. In this study, the inversion is performed using an iteratively reweighted least squares approach (Farquharson and Oldenburg, 1998), where a Taylor expansion of the objective function is used to form the model update. Within this framework alternative stabilizer functions are implemented by reweighting the roughness matrix within an L_2 norm (Vignoli et al., 2015; Fiandaca et al., 2015).

The MGS stabilizer (also referred to as focused or sharp inversion) provides the benefits of the many layer inversion but while maintaining the ability to produce models with sharp contrasts in properties (Portniaguine and Zhdanov, 1999). Briefly, the minimum gradient support stabilizer penalizes the number of sharp contrasts in the model regardless of their magnitude allowing the production of models with sharp interfaces between layers of relatively homogenous properties. The MGS stabilizer has been demonstrated to improve image sharpness for many layer inversion schemes in magnetic

(Portniaguine and Zhdanov, 1999), gravity (Portniaguine and Zhdanov, 1999), TEM (Vignoli et al., 2015), ERT (Pagliara and Vignoli, 2006), magentoteullurics (Zhdanov and Tolstaya, 2004), seismic (Zhdanov et al., 2006) and IP (Blaschek et al., 2008) studies. An additional stabilizer, employing an L_1 norm (instead of the L_2 norm present in the smoothness stabilizer) is also investigated. The L_1 norm penalizes the absolute value of the variation in model parameters. This allows for sharper contrasts in model parameters compared to the smoothness stabilizer (Loke et al., 2003), but not as readily as the MGS stabilizer. Mohnke and Yaramanci (2002) found that surface NMR inversions that use an L_1 stabilizer are better suited to producing models with sharp contrasts compared to the smoothness stabilizer. The L_1 norm is included in this comparison to compare its performance with the MGS stabilizer because of its ease of use. Synthetic results are presented to investigate the performance of each stabilizer for surface NMR inversion in the presence of a layered subsurface. Results of the many layer inversions are also compared against a few layer inversion. Discussion about the implementation of alternative stabilizers into existing inversion packages and guidelines for the use of the MGS stabilizer are also given.

BACKGROUND

The Surface NMR Inverse Problem

The standard measurement in surface NMR is the free induction decay, which involves measurement of the NMR signal following a single current pulse. To investigate the spatial variability of aquifer properties, the amplitude of the current pulse is altered to manipulate the spatial origin of the measured signal. The forward model is given by

$$\mathbf{d} = g(\mathbf{m}) + \mathbf{e}, \quad (1)$$

where **d** is a vector containing the measured NMR decays (for all current amplitudes for all time samples), and **m** is a vector containing the model parameters (water contents and T_2^* in each depth layer). For a many layer inversion the number of depth layers, and their thicknesses are predetermined. For a few layer inversion the model **m** also contains the layer thicknesses. The *g* function describes the physics of the forward problem; it contains: 1) information about the expected spatial origin of the measured signal corresponding to the excitation pulse type, current amplitude, and pulse duration, 2) a spatial weighting based on the receiver sensitivity at each location in the subsurface, 3) the impact of a conductive subsurface on depth penetration and signal phase, and 4) a scaling parameter to estimate the magnitude of the equilibrium magnetization given the local magnetic field strength (local Earth's field strength) and aquifer temperature. **e** is a vector of the noise present in the data. Detailed derivation of the surface NMR forward model is given in Weichman et al. (2000).

To estimate the spatial distribution of aquifer properties an inversion is used to predict the model that balances satisfactory data fit with the magnitude of the regularization term. To determine this model an objective function $\Phi(\mathbf{m})$, described by

$$\Phi(\mathbf{m}) = \phi_d(\mathbf{m}) + \phi_s(\mathbf{m}), \qquad (2)$$

is minimized. The $\phi_d(\mathbf{m})$ term describes the L_2 norm misfit between the predicted data ($g(\mathbf{m})$) and the observed data (normalized by the data uncertainty), while $\phi_s(\mathbf{m})$ is the stabilizer function that determines the magnitude of the regularization term for the current model **m**. The $\phi_d(\mathbf{m})$ term is given by

$$\phi_d(\mathbf{m}) = \|\mathbf{Q}_d(\mathbf{d} - g(\mathbf{m}))\|_{L_2}^2, \ (3)$$

where $\mathbf{Q}_\mathrm{d}^\mathrm{T}\mathbf{Q}_\mathrm{d} = \mathbf{C}_\mathrm{d}^{-1}$, i.e. the inverse of the data covariance matrix. The stabilizer function is described by

$$\phi_s(\mathbf{m}) = \left\|\mathbf{Q}_{\boldsymbol{R}}\,\mathbf{Rm}.\ \right\|_{\eta}^{2}, with\ \eta = L_2\ or\ L_1\ or\ MGS, \ (4a)$$

and is necessary to stabilize the ill-posed inversion by penalizing models that exhibit undesired traits. $\mathbf{Q}_\mathbf{R}$ is a matrix used to weight the relative importance of the stabilizer function for each model constraint; $\mathbf{Q}_\mathrm{R}^\mathrm{T}\mathbf{Q}_\mathrm{R} = \mathbf{C}_\mathrm{R}^{-1}$, where $\mathbf{C}_\mathrm{R}$ is a matrix containing the variances of the constraints. The **R** matrix is called the roughness matrix, and is used to calculate the first order difference between the model parameters in neighboring depth layers. The η parameter corresponds to the norm used by the stabilizer (L_2 or L_1 or MGS). In this study the different norms are implemented using a reweighting matrix **W**(**m**) and an L_2 norm, where the stabilizer function is given by

$$\phi_S(\mathbf{m}) = \left\|\boldsymbol{Q}_{\boldsymbol{R}}\, \mathbf{W}(\mathbf{m})\mathbf{Rm}.\ \right\|_{L_2}^2 . (4b)$$

The form of **W**(**m**) corresponds to the specific norm desired and can be determined by equating equation 4b with the equations describing the stabilizers in the following section. Equation 4b indicates that selection of a norm different than L_2 (the smoothness case) does not require significant modifications to existing inversion codes, it only requires the inclusion of an additional weighting matrix within the stabilizer.

To find the model **m** that minimizes equation 2 an iteratively reweighted least squares approach is used (Farquharson and Oldenburg, 1998), where the Taylor expansion of the objective function is used to determine the model update. This involves updating the estimated model iteratively; ultimately converging on a model that minimizes the objective function. Details about the inversion scheme employed in this manuscript are given in Auken et al., (2004), Vignoli et al. (2015), and Fiandaca et al. (2015). Note that the objective function (equation 2) does not contain a trade-off parameter that can be used to weight the relative importance of the ϕ_d and ϕ_s terms (the trade-off parameter is typically denoted by λ). The inversion scheme used in this study weights these terms equally, where the importance of the stabilizer term is controlled through the $\mathbf{Q_R}$ matrix that weights the relative importance of the stabilizer for each model parameter.

Selecting a stabilizer function

The stabilizer function stabilizes the inversion and allows the production of models with a desired property. This is done by penalizing models that exhibit an undesired trait. Equations 5a, 5b, and 5c illustrate the equations for a smoothness (L_2) stabilizer (the standard stabilizer in surface NMR inversions), the L_1 stabilizer, and the minimum-gradient support stabilizer, respectively:

$$\phi_s(\mathbf{m}) = \sum_k \left(\frac{(\Delta\mathrm{m})_k}{\sigma_k}\right)^2. \quad (5a)$$

$$\phi_s(\mathbf{m}) = \sum_k \sqrt{\left(\frac{(\Delta\mathrm{m})_k}{\sigma_k}\right)^2}. \quad (5b)$$

$$\phi_s(\mathbf{m}) = \frac{1}{\beta}\sum_k \frac{\left(\frac{(\Delta\mathrm{m})_k}{\sigma_k}\right)^2}{\left(\frac{(\Delta\mathrm{m})_k}{\sigma_k}\right)^2+1}, \quad (5c)$$

The $(\Delta\mathrm{m})_k$ term corresponds to the first order difference of the constrained parameters for the k^{th} constraint; i.e. $(\Delta\mathrm{m})_k = \mathrm{m}_{j(k)}-\mathrm{m}_{i(k)}$, where j(k) and i(k) represent the indices in the model vector of the parameters linked through the k^{th} constraint. For the L_2 and L_1 stabilizers the σ_k term represents the strength of the constraint, because it controls the relative importance in the stabilizer function for the k^{th} constraint. Equation 5a indicates that the smoothness $\phi_s(\mathbf{m})$ increases proportional to square of the difference between neighboring model parameters. As such, sharp variations result in larger $\phi_s(\mathbf{m})$ and larger $\Phi(\mathbf{m})$. The minimization will therefore return smoothly varying models, as models with sharp transitions will be penalized. The L_1 stabilizer (Equation 5b) penalizes the absolute value of the difference in model parameters instead of the square of difference. As a result, smoothly varying models are still favored by the L_1 norm but sharp variations are penalized much less compared to the smoothness stabilizer. For both the L_2 and L_1 stabilizers , selection of σ_k controls the smoothness of the final model; large σ_k places little importance on the smoothness allowing more erratic profiles to be produced in order to further minimize $\phi_d(\mathbf{m})$, while small σ_k places more importance on model smoothness at the expense of a larger data misfit.

If a priori knowledge suggests sharp transitions are likely at a particular site, selection of a smoothness stabilizer is suboptimal given that it penalizes models with characteristics expected to be representative of the local hydrogeology. In this case, an alternative stabilizer may provide improved performance. For example, the minimum gradient support stabilizer (Portniaguine and Zhdanov, 1999) presents a more efficient implementation of a priori knowledge of blocky structures. In this case, $\phi_s(\mathbf{m})$ is given by equation 5c; the form of the MGS stabilizer in equation 5c is chosen to be consistent with Vignoli et al., 2015. This form of the MGS stabilizer presents a parameterization allowing a simple understanding of the physical meaning of β and σ_k. Consider the effect of the MGS stabilizer in three regimes. In the $\left(\frac{(\Delta \mathrm{m})_k}{\sigma_k}\right)^2 \gg 1$ limit, which describes the sharp change in model parameters at the interface between layers of contrasting properties, the contribution to $\phi_s(\mathbf{m})$ approaches $1/\beta$. Therefore, the presence of a sharp transition in the model parameters is not penalized based on the magnitude of the model variation (as in the smoothness case) but rather penalized a fixed amount. In the $\left(\frac{(\Delta \mathrm{m})_k}{\sigma_k}\right)^2 \approx 1$ regime the contribution to $\phi_s(\mathbf{m})$ scales approximately with the square of the difference in model parameters. In the $\left(\frac{(\Delta \mathrm{m})_k}{\sigma_k}\right)^2 \ll 1$ regime there is little penalization and the contribution to $\phi_s(\mathbf{m})$ is small. This indicates that the MGS stabilizer will not severely penalize models containing sharp transitions, but will search for models with as few sharp transitions as possible with relatively homogenous properties between these sharp transitions (Portniaguine and Zhdanov, 1999). σ_k and β effectively control the extent of homogeneity within a layer, and the number of sharp transitions present in the final model, respectively. The value of β does not directly control to the number of sharp transitions present in the estimated model, but its magnitude does influence the number of transitions present. Models corresponding to large values of β have more transitions than models with small β.

Implementation of each norm in this study is done using the weighting matrix $\mathbf{W}(\mathbf{m})$, determined by equating equation 4b with equation 5a, 5b, or 5c. Note that for the L_1 and MGS stabilizers

W(**m**) depends on the current model, requiring that **W**(**m**) be recalculated every iteration. The computational cost of updating **W**(**m**) is not significant and each inversion proceeds at similar speeds in the case of a 1D surface NMR sounding. The stabilizer can also take other forms to describe different a priori conditions. In this manuscript the L_1 and MGS stabilizers are selected based on their less severe penalization of models containing sharp transitions in model parameters compared to the smoothness stabilizer.

RESULTS

Three synthetic surveys are presented to compare the utility of the L_1 and MGS stabilizers against the smoothness stabilizer for many layer surface NMR inversions. Each stabilizer is also compared against the results of a few layer inversion. Forward modelling and inversion of the synthetic data is performed using the AarhusInv software package (Auken et al., 2015), following the Behroozmand et al. (2012) forward implementation. The inversion is performed using the amplitudes of the NMR signals (i.e. the in and out of phase components of the data are not treated separately). The inversion also bounds the estimated water contents to fall between 0.1% and 100%, while the relaxation times are bound between 5ms and 1.5 s. In each case FID measurements are simulated using a coincident transmit/receive 100 m square loop, a 30 ms on-resonance excitation pulse and 16 pulse moments sampled on the interval from 0.7 As to 8.5 As. The selected pulse moments are chosen to span a range typical of surface NMR field experiments. The subsurface resistivity is 1000 Ωm in each case, and is fixed during the inversion. This is equivalent to the inversions having a priori knowledge of the exact subsurface resistivity structure; a simple resistive subsurface is chosen to focus the comparison on the ability to estimate the subsurface parameters common to all surface NMR inversions (water content and relaxation times). In practice it is common for non-joint NMR-TEM inversion schemes to treat the subsurface resistivity structure (estimated form a separate TEM or other electrical survey) as fixed during the inversion. The Larmor frequency is set to 2138

Hz. Each inversion begins with a starting model corresponding to a half space of 15% water content and T_2* of 150 ms. The data are binned into 12 time gates of logarithmically increasing width. The earliest and latest time gates are centered at 41 ms and 445 ms, respectively. Gaussian white noise is added to the time gated data. To account for the varying widths of the time gates, the noise added to each time gate is scaled by the square root of the ratio of the time gate's width compared to the width of the first time gate. The stated noise levels refer to the standard deviation of the Gaussian used to generate the noise in the first time gate (width of the first time gate is 7.1 ms). The subsurface is discretized into 25 depths of increasing thickness to a depth of 110 m. The shallowest layers have thicknesses of 1.5 m and increase to a thickness of ~10m (layer thicknesses increase roughly logarithmically). Below 110m the subsurface is treated as a halfspace. A model discretization consisting of 25 depth layers was chosen to balance the opportunity to capture smoothly varying parameters without dramatically over parameterizing the subsurface. Increasing the number of depth layers places more importance upon the regularization. Further discussion about the approach used to discretize the subsurface is given in Behroozmand et al. (2012). Note that the layer boundaries for the synthetic subsurface models occur at the same depths as layer interfaces in the model discretization. In practice the depth discretization is unlikely to coincide with the true layer boundaries, in this case it would cause either smearing between two layers, or an error in identifying exact depth of the interface.

In each example, 200 noisy data sets are produced by adding different noise realizations to the same noise free data set. For the first three examples the noise level is 20 nV (i.e. the standard deviation of the Gaussian used to randomly generate noise for the first time gate is 20 nV). Although the signal to noise ratio (SNR) in each case depends on the subsurface model, this level of noise produces an SNR of ~50-80 for the three examples. For each noisy data set a water content and T_2* profile is estimated using a many layer inversion with a smoothness stabilizer, a many layer inversion with an L_1 stabilizer, a many layer inversion with an MGS stabilizer, and a few layer inversion. The 200 estimated water content and T_2* profiles produced by each inversion scheme are used to form histograms of the water content and T_2* values in each depth layer. The top two rows of Figure 1 illustrate several examples of how the histograms will be illustrated. The y-axes correspond to depth, the x-axes to either water content or T_2*, and the color scale indicates the number of counts present in each bin (black indicates a high number of counts and white indicates no counts). The water content and T_2* bins are 0.5% and 5 ms wide, respectively. The histograms allow the uncertainty of the resulting profiles to be estimated by examining the distribution of water contents and T_2* values within each depth layer. Low and high uncertainty correspond to depth layers with narrow black distributions and wide light grey distributions, respectively. Note that the histograms do not illustrate the full range of equivalent solutions as each inversion begins with the same starting model. However, the histograms remain a useful tool to provide insight into the uncertainty in the estimated profiles. For each stabilizer the results for single regularization strength are shown. The strength of the regularization is selected to produce the smoothest model that fits the data within error. The constraint strengths σ_k used in this study are relative to the magnitude of the model parameter $m_{i(k)}$; i.e. the constraint strength is effectively controlled by a parameter denoted σ_{rel}, where σ_k=(σ_{rel}m $_{i(k)}$- $m_{i(k)}$). The inversion in this study is carried out in logarithmic model space, therefore $(\Delta \mathrm{m})_k$ becomes $log(\mathrm{m}_{j(k)}) - log(\mathrm{m}_{i(k)})$ and σ_k is estimated by subtracting the log-transformed parameter from the log-transformed upper limit of its confidence interval, i.e. σ_k becomes $log(\mathrm{m}_{i(k)} + \sigma_k) - log(\mathrm{m}_{i(k)})$. Therefore, the penalty $p = \frac{(\Delta \mathrm{m})_k}{\sigma_k}$ of equations 5a-c can be expressed in terms of σ_{rel} as $p = \frac{log(\mathrm{m}_{j(k)}) - log(\mathrm{m}_{i(k)})}{log(\mathrm{m}_{i(k)} - (\sigma_{rel}-1)\cdot \mathrm{m}_{i(k)}) - log(\mathrm{m}_{i(k)})} = \frac{log\left(\mathrm{m}_{j(k)}/\mathrm{m}_{i(k)}\right)}{log(\sigma_{rel})}$.. For example, σ_{rel}=1.1 means model parameter variations of ~10% is acceptable (i.e. should not be penalized severely). Given the noise level of 20 nV, σ_{rel}=1.5 was used for the smoothness and L_1 stabilizers, while for the MGS stabilizer σ_{rel}=1.1 and β=50. Note that for each stabilizer the water contents and T_2* parameters are given the same constraint strengths. Further discussion about the selection of the MGS stabilizer parameters is given in the discussion.

Figures 1, 3 and 4 contrast the performance of each stabilizer. The top row in each figure illustrates the estimated water content profiles, the middle row the estimated T_2* profiles, and the bottom row shows a histogram of the resulting χ^2 in each case. χ^2 is unitless, as the data misfit (nV) is normalized by the data uncertainty (nV). χ^2 histograms clustered around 1 indicate good data fit (χ^2 is close to 1 because it is normalized by the number of data points). Columns one to three correspond to a many layer inversions that use a smoothness stabilizer, a L_1 stabilizer, and a MGS stabilizer, respectively. Column four illustrates the results of a few layer inversions that is given the correct number of layers. The true water content and T_2* profiles in each case are illustrated by the red dashed lines.

The first example (Figure 1) is a three layer system containing a single aquifer. The aquifer is 14 m thick (from 11-25 m depth) with a water content of 40% and T_2*=200 ms. The layers above and below this aquifer have reduced water content (5%) and faster T_2* (50 ms). The smoothness inversion (left column) accurately resolves the increased water content and T_2* layer producing reliable estimates of the water content and T_2* magnitudes in all three layers. The large contrast at the upper boundary is well-resolved by the smoothness stabilizer, while the lower boundary is smoothed over a larger depth range. The L_1 stabilizer (column 2) resolves the properties of all three layers well, capturing the sharp contrast at the upper layer boundary while also estimating a sharper transition to low water content and T_2* at the lower layer boundary compared to the smoothness stabilizer. The MGS stabilizer (column 3) produces similar results as the L_1 stabilizer and resolves both layer boundaries well. The estimated water contents and T_2* within the aquifer (layer 2) show less variation for the MGS case than the L_1 and smoothness stabilizer cases (darker narrower histograms). The few layer inversion, which was given the correct number of layers a priori, accurately reproduces the true model. In this example, the blocky true model is reproduced with high precision by the L_1, MGS, and few layer inversions, while the smoothness results make the identification the lower layer boundary more difficult. The bottom column of Figure 1 indicates that each inversion approach was able to fit the data to similar levels, with the data residual norms clustered around one. To give an example of the noisy data and quality of data fit Figure 2 illustrates the first of the two hundred noisy data sets (left panel) and the data residual (right panel) produced by the MGS stabilizer. The residual shows no structure (i.e. no large areas with consistent sign) and has a magnitude consistent with the noise level. The χ^2in this example is 1.02. Figure 2B is representative of the residual produced by inversions resulting in similar magnitude χ^2.

The second example (Figure 3) is a slightly more complicated four layer system containing two aquifers. The two aquifers (layers 1 and 3) have water content of 30% and T_2*=200 ms. The layer separating these aquifers and the bottom layer have reduced water content (5%) and T_2* (50 ms). In this case, the smoothness inversion (left column) produces a smoothed version of the layered subsurface. The water content and T_2* are well estimated in each layer, but it is difficult to identify the layer boundaries given the smooth variations. For example, the upper and lower layer boundaries for layer 3 (the lower aquifer) are both spread over a 5-10m depth range. The L_1 inversion also reproduces the water content and T_2* magnitudes well, while better identifying the boundaries between the upper three layers. The MGS stabilizer produces similar results as the L_1 stabilizer, but with the lower boundary between layer 3 and 4 being more sharply resolved. The water content and T_2* values estimated within layers 1 and 3 are also more homogenous than the L_1 stabilizer (observed by narrower darker histograms for the MGS case compared to the L_1 case). Both the L_1 and MGS stabilizers struggle to resolve the magnitude of T_2* in the second layer. This is a consequence of the low water content at these depths which reduces the ability to resolve the magnitude of T_2*. For the few layer inversion, which is given the correct number of layers, the true model is well reproduced. The estimated T_2* value in layer 2 also has higher uncertainty (noted by the wide histogram). Overall, the few layer result is quite similar to that produced by the MGS stabilizer, with each layer boundary being well resolved. The L_1 and smoothness inversions are less able to capture the large contrast in properties at the lower boundary between layer 3 and 4. The bottom row of Figure 3 indicates that each inversion provides a similar level of data fit.

The third example (Figure 4) tests the performance of each stabilizer given a subsurface containing a smooth variation in water content. In this case the water content is 10% at the shallowest depth and increases roughly linearly to 40% at 37 m depth; T_2* is equal to 100 ms at all depths. Below 37m a homogenous 40% water content layer is present. The smoothness inversion (left column) accurately captures the slowly increasing water content profile, while estimating a smooth transition to lower water content at depth (below ~37 m). The L_1 stabilizer produces similar results as the smoothness case, capturing the smoothly increasing water content profile while better predicting a homogeneous water content below 37 m (narrow dark histograms). The MGS stabilizer also reproduces the true model well, with a similar prediction of the homogeneity below 37 m as the L_1 stabilizer. The T_2* profile is well resolved in all cases, except at the shallowest depths.. The systematic bias towards underestimated T_2* at the shallowest depths likely results from the T_2* at these depths having little impact on the overall data fit (given that these depths correspond to the lowest water contents). For the few layer inversion results, where the inversion is given 5 layers, a blocky stepwise increasing water content is predicted, with the overall structure in the water content being captured. The water contents at depths above ~37 m are more uncertain for the few layer inversion compared to the many layer inversions (wide light grey histograms). Below 37 m the few layer inversion accurately estimates the water content. The bottom row of Figure 4 indicates that each inversion scheme produces similar levels of data fit. For some noise realizations χ^2 is large (>~1.3) and the data fit is reduced. While increasing the number of layers for the few layer inversion will improves its ability to capture the smooth change in water content, the 5 layer model is shown given the preference for the model containing the fewest number of layers that provides satisfactory data fit.

Figures 1, 3, and 4 illustrate that the smoothness stabilizer is suboptimal when sharp layer boundaries are expected and the selection of an alternative stabilizer can improve the performance of the many layer inversion in the presence of a layered subsurface. Comparing the L_1 and MGS results indicates that the MGS stabilizer provides the best ability to reproduce a blocky subsurface structure when using a many layer inversion. Even in a smoothly varying subsurface, the MGS stabilizer produces a reliable result.

The benefit of the MGS stabilizer is that it is able to resolve blocky structures without requiring knowledge of the number of layers a priori; the MGS results even provides similar performance to a few layer inversion given the correct number of layers. Note that for the depth discretization and noise levels used in these examples, a fixed level of regularization for the MGS stabilizer can be expected to provide flexible performance capable of resolving both smoothly varying and blocky subsurface structures. The few layer inversion also performs well for a layered subsurface provided that a sufficient number of layers is used in the inversion.

DISCUSSION

The selection of a many layer versus few layer inversion scheme should consider the available a priori information about the site. If little information about the subsurface is present, such as whether a layered or smoothly varying subsurface is present, the many layer inversion offers the benefits requiring no a priori specification about the number of layers. A preliminary many layer inversion can also be used to inform a subsequent few layer inversion, where the many layer result can be used to provide an initial model and helps in choosing the number of layers for the few layer inversion. Whether the result of the many layer inversion is to be used as the final estimated model or as a starting model for a few layer inversion it is beneficial to use a stabilizer well suited to producing models with features consistent with the expectations of the subsurface. Therefore, if a layered subsurface is expected the standard smoothness stabilizer is suboptimal. Both the L_1 and MGS stabilizer improve the ability of the many layer inversion to reproduce blocky structures. However, results produced by a many layer that uses an L_1 or MGS stabilizer are not necessarily more accurate than those produced by a smoothness stabilizer. Given equal levels of data fit, the results produced by each stabilizer represent equally-likely models. Similarly, few layer inversions providing similar data fits as the many layer inversion also provide equally-likely models. To decide between the potential models additional geologic information should be considered, such as the depositional environment which may help inform whether a layered or smoothly varying subsurface is more likely. The advantages of the L_1 and MGS stabilizer is that they provide a means for the many layer inversion to more readily produce sharp contrasts in properties.

Practical Considerations for using the MGS stabilizer in surface NMR

We now focus on the MGS stabilizer given that it provides the best ability to reproduce a layered subsurface when using a many layer inversion. The contribution of the MGS stabilizer to the objective function is controlled by two parameters, σ_k and β. In contrast, the smoothness and L_1 stabilizers are controlled by a single parameter σ_k. The additional parameter for the MGS stabilizer complicates the decision as to how the regularization strength should be selected. For the smoothness and L_1 cases the general rule for selection of the regularization strength is that the smoothest model producing satisfactory data fit should be selected, otherwise the inversion may introduce spurious features into the estimated profiles in an attempt to over fit the data. For the MGS stabilizer, selection of σ_k and β requires balancing the desired level of homogeneity within a layer with the number of sharp contrasts present in the estimated models. To illustrate the impact of each parameter on the performance of the MGS stabilizer Figure 5 shows the water content profiles for MGS inversions performed with different combinations of σ_{rel} and β given the same suite of 200 noisy data sets used to form Figure 3 (the two aquifer system). Each row and column corresponds to a particular σ_{rel} and β, respectively. The top middle panel is a reproduction of the MGS water content profiles from Figure 3. For small σ_{rel} (top row) the intralayer homogeneity is high, noted by dark narrow histograms. For larger σ_{rel} (rows 2 and 3), the intralayer homogeneity is reduced (wider light grey histograms) and the results begin to more closely resemble the smoothness water content profile in Figure 3. For increasing β (left column to right column) the likelihood of additional sharp contrasts is increased. In this example, this results in a blurring of the layer boundaries due to the reduced penalization of additional sharp contrasts in the final model. At this noise level (20 nV) each level of regularization fits the data to similar levels, except for the top left panel which produces a slightly poorer data fit. Given that the motivation to use an MGS stabilizer is to improve the ability of the many layer inversion to reproduce a layered subsurface, we recommend selecting a low σ_{rel} value (eg. fixing σ_{rel} to 1.1). This ensures that relatively homogeneous layers are produced, and effectively allows the regularization strength to be controlled by specifying a β value. The selected β should be as small as possible while still providing satisfactory data fit. For the depth discretization and noise levels used in these examples β=50 was observed to provide good performance. The corresponding T_2* profiles (for the same σ_{rel} and β pairs) exhibit similar trends (not shown).

Choosing the regularization strength also depends upon the signal to noise ratio. To investigate the performance of the MGS stabilizer for varying noise conditions Figure 6 illustrates the water content and T_2* profiles estimated using a many layer inversion with an MGS stabilizer for noise levels of 20, 50, and 75 nV. The true subsurface model in this example is the same as Figure 3. These noise levels roughly correspond to SNR of ~60, ~25, and ~15, respectively. At the lowest noise condition (20 nV) the true subsurface model is well reproduced, except for the T_2* value in layer 2. For noise levels of 50 and 75 nV, the estimated water content and T_2* profiles have larger uncertainty (wider light grey histograms) and no longer resolve the T_2* contrast between layer 2 and its neighbors. The data fit is also reduced at higher noise levels (as illustrated by the χ^2 histograms in the bottom row of Figure 6). In several cases with higher χ^2 the data residual plots show structure indicating a poor data fit. In these cases, the estimated profiles would be treated with high uncertainty. Note that the histograms effectively hide these poor profiles, as they are only 1 of 200 results. In practice, a high noise level may cause the MGS stabilizer to predict a sharp boundary at an incorrect depth or where no contrast exists at all. In this limit it may be preferable to use the MGS stabilizer to inform the number of depth layers present and to use this information as the a priori number of layers for a subsequent few layer inversion. The few layer inversion can then be used to readily quantify the uncertainty in the estimated profiles. Alternatively, in the high noise limit it may be preferable to use the smoothness inversion given that strong smoothness regularization may limit the introduction of spurious sharp contrasts (at the expense of resolving layer boundaries). At noise levels greater than that investigated in Figure 6 (which may happen depending on local noise conditions) the profiles show even greater uncertainty.

The σ_k and β parameters also depend on the depth discretization used in the many layer inversion. As such, we recommend that synthetic studies with similar models to those considered in Figures 1, 3, and 4 be performed using the same depth discretization that which will be used in the inversion of field data and with noise levels similar to the field data. This will help inform the range of σ_k and β parameters likely to provide satisfactory performance and will provide insight into how capable the inversion is of resolving a synthetic model with features similar to those present in the water content and T_2* profiles produced by the field data. Similar synthetic tests would also help select a regularization strength and understand the resolution of the final models for the smoothness and L_1 stabilizers.

CONCLUSIONS

The ability of the many layer surface NMR inversion to reproduce a layered subsurface is compared for several stabilizer functions. The standard stabilizer (smoothness stabilizer) penalizes sharp transitions in subsurface properties and is poorly suited to imaging layered subsurfaces. Two alternative stabilizers, an L_1 stabilizer and minimum-gradient support stabilizer, were found to improve the ability to identify sharp contrasts in layer properties. The minimum gradient support stabilizer is observed to greatly improve the ability of the many layer inversion to reproduce blocky structures. Although the L_1 norm is observed to also provide improved performance compared to the smoothness approach for layered subsurfaces, its improvement is less than the MGS stabilizer. Improving the utility of the many layer inversion in a layered environment benefits both the scenario where the model produced by the many layer inversion is used for building the conceptual model of the subsurface and the scenario where the many layer inversion is used to build an initial model and an estimate of the number of layers needed for a subsequent few layer inversion.

The form of the MGS stabilizer employed in this study provides a simple understanding of the role played by the two tunable parameters in the stabilizer function. The extent of water content and T_2* homogeneity within a layer for the MGS stabilizer is controlled by σ_k (we recommend that variations greater than 10% be penalized), while the number of sharp transitions present in the final model is influenced by β (small and large β lead to less and more transitions, respectively). Despite two tunable parameters, selection of appropriate inversion parameters is straightforward and a single set of parameters is observed to provide accurate results for a broad range of subsurface models. For the inversion of field data we recommend selecting inversion parameters based on observations from synthetic tests with simple models (like those present in Figures 1-4), the same model discretization, and similar noise conditions as the field data. In high noise conditions it may be preferable to use the MGS many layer inversion to inform a few layer inversion, allowing the uncertainty of the estimated profiles to be more readily quantified. Alternatively, the standard smoothness stabilizer may be preferable to the MGS stabilizer in high noise environments in order to limit the introduction of spurious sharp contrasts that may be interpreted as layer boundaries. However, this comes at the expense of resolving sharp contrasts. In summary, the minimum gradient support stabilizer provides an effective means to improve the flexibility of the many layer surface NMR inversions.

ACKNOWLEDGEMENTS

Denys Grombacher was supported by funding from a Danish Council for Independent Research Postdoctoral Grant (DFF-5051-00002). Ahmad A. Behroozmand was partly supported by funding from the Danish Council for Independent Research.

REFERENCES

Auken, E. and Christiansen, A.V. 2004. Layered and laterally constrained 2D inversion of resistivity data. Geophysics, 69 (no. 3), 752-761.

Auken, E., Christiansen, A.V., Kirkegaard, C., Fiandaca, G., Schamper, C., Behroozmand, A.A., Binley, A., Nielsen, E., Effersø, F., Christensen, N.B., Sørensen, K., Foged, N., and Vignoli, G. 2015. An overview of a highly versatile forward and stable inverse algorithm for airborne, ground-based, and borehole electromagnetic and electric data. Exploration Geophysics 46 (no. 3), 223-235.

Behroozmand, A.A., Auken, E., Fiandaca, G. and Christiansen, A.V. 2012. Improvement in MRS parameter estimation by joint and laterally constrained inversion of MRS and TEM data. Geophysics 77 (no. 4), WB191-WB200.

Blaschek, R., Hordt, A. and Kemna, A. 2008. A new sensitivity-controlled focusing regularization scheme for the inversion of induced polarization data based on the minimum gradient support. Geophysics 73 (no. 2), F45-F54.

Ellis, R.G. and Oldenburg, D.W. 1994. Applied geophysical inversion. Geophysical Journal International 116, 5-11.

Farquharson, C.G. and Oldenburg, D.W. 1998. Non-linear inversion using general measures of data misfit and model structure. Geophysics 134, 213-217.

Fiandaca, G., Doetsch, J., Vignoli, G., and Auken, E. 2015. Generalized focusing of time-lapse changes with applications to direct current and time-domain induced polarization inversions. Geophysical Journal International 203 (no. 2), 1101-1112.

Guillen, A., and Legchenko, A. 2002. Inversion of surface nuclear magnetic resonance data by an adapted Monte Carlo method applied to water resource characterization. Journal of Applied Geophysics 50, 193-205.

Günther, T., and M. Müller-Petke, 2012. Hydraulic properites at the North Sea island of Borkum derived from joint inversion of magnetic resonance and electrical resistivity soundings. Hydrology and Earth System Sciences 16 (no. 9), 3279-3291.

Hertrich, M. 2008. Imaging of groundwater with nuclear magnetic resonance. Progress in Nuclear Magnetic Spectroscopy 53, 227-248.

Irons, T.P., and Li, Y. 2014. Pulse and Fourier transform surface nuclear magnetic resonance: comprehensive modeling and inversion incorporating complex data and static dephasing dynamics. Geophysical Journal International 199, 1372-1394.

Last, B.J., and Kubik, K. 1983. Compact gravity inversion. Geophysics 48 (no. 6), 713-721.

Legchenko, A., and Valla, P. 2002. A review of the basic principles for proton magnetic resonance sounding measurements. Journal of Applied Geophysics 50, 3-19.

Loke, M.H., Acworth, I. and Dahlin, T. 2003. A comparison of smooth and blocky inversion methods in 2D electrical imaging surveys. Exploration Geophysics 34, 182-187.

Mohnke, O., and Yaramanci, U. 2002. Smooth and block inversion of surface NMR amplitudes and decay times using simulated annealing. Journal of Applied Geophysics 50 (no. 1-2), 163-177.

Müller-Petke, M., and Yaramanci, U. 2010. QT inversion—Comprehensive use of the complete surface NMR data set. Geophysics 75 (no. 4), WA199-WA209.

Pagliara, G., and Vignoli, G. 2006. Focusing inversion techniques applied to electrical resistance tomography in an experimental tank. Proceedings of the 11th International Congress of the International Association for Mathematical Geology.

Portniaguine, O. and Zhdanov, M.S. 1999. Focusing geophysical inversion images. Geophysics 64 (no. 3), 874-887.

Schriov, M., Legchenko, A. and Creer, G. 1991. A new direct non-invasive groundwater detection technology for Australia. Exploration Geophysics 22 (no. 2), 333-338.

Tikhonov, A. N., and Arsenin, V. Y. 1977. Solutions of ill-posed problems. Washington, D.C., Winston.

Vignoli, G., Fiandaca, G., Christiansen, A.V., Kirkegaard, C. and Auken, E. 2015. Sharp spatially constrained inversion with applications to transient electromagnetic data. Geophysical Prosepcting 63, 243-255.

Weichman, P.B., Lavely, E.M. and Ritzwoller, M.H. 2000. Theory of surface nuclear magnetic resonance with applications to geophysical imaging problems. Physical Review E 62, 1290-1312.

Weichman, P.B., Lun, D.R., Ritzwoller, M.H. and Lavely, E.M. 2002. Study of surface nuclear magnetic resonance inverse problems. Journal of Applied Geophysics 50 (no. 1-2), 129-147.

Zhdanov, M., and Tolstaya, E. 2004. Minimum support nonlinear parameterization in the solution of a 3D magentotelluric inverse problem. Inverse Problems 20 (no. 3), 937-952.

Zhadnov, M.S., Vignoli, G. and Ueda, T. 2006. Sharp boundary inversion in crosswell travel-time tomography. Journal of Geophysics and Engineering 3 (no. 2), 122-134.

FIGURES AND FIGURE CAPTIONS

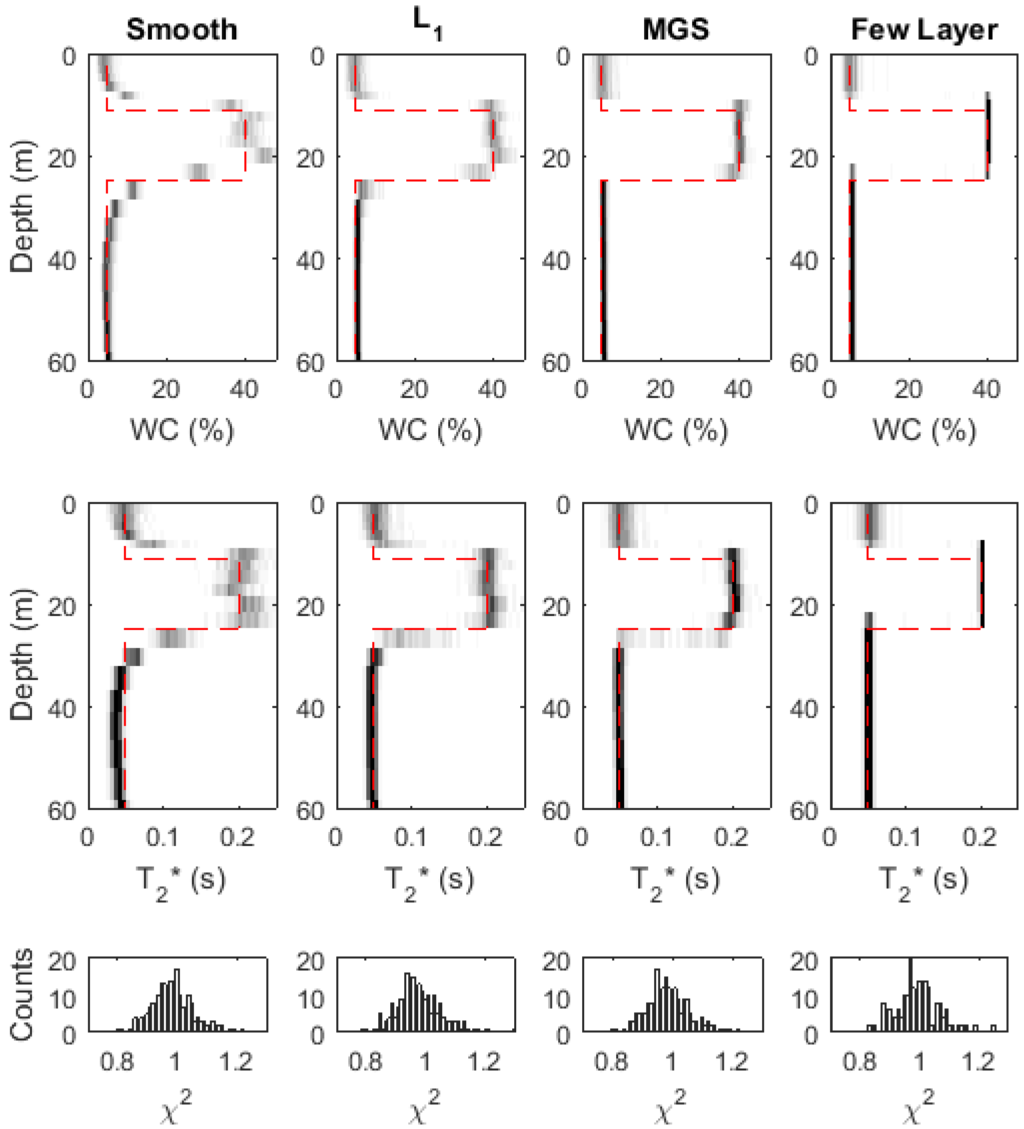

Figure 1. Histograms showing the water content (WC) (top row) and T_2* profiles (middle row) estimated from the inversion of 200 independent noisy data sets. The bottom row illustrates a histogram of the χ^2 for all 200 inversions. The dashed red line shows the true model (a three layer system with a single aquifer). Dark and white colors indicate bins with many and no counts, respectively. Columns left to right show the results for a many layer inversion using a smoothness stabilizer, a many layer inversion using an L_1 stabilizer, a many layer inversion using a MGS stabilizer, and a few layer inversion with 3 layers. The noise level is 20 nV. Black and white bins have 70 and 0 counts, respectively.

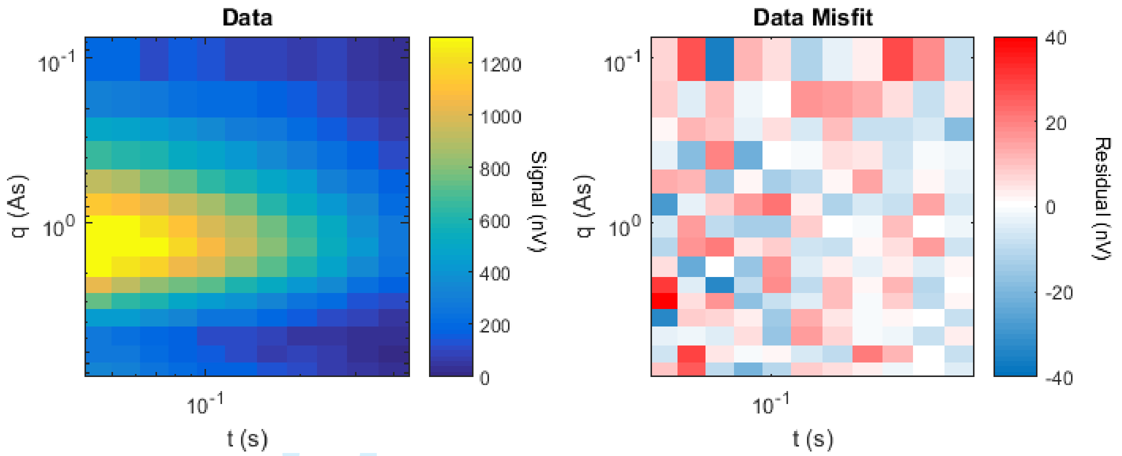

Figure 2. A) One of the 200 noisy data sets produced by the subsurface model in Figure 1. B) An example of the data residual produced by the many layer inversion using the MGS stabilizer. This data residual corresponds to a χ^2 of 1.02 and is representative of that produced by other inversions with similar χ^2.

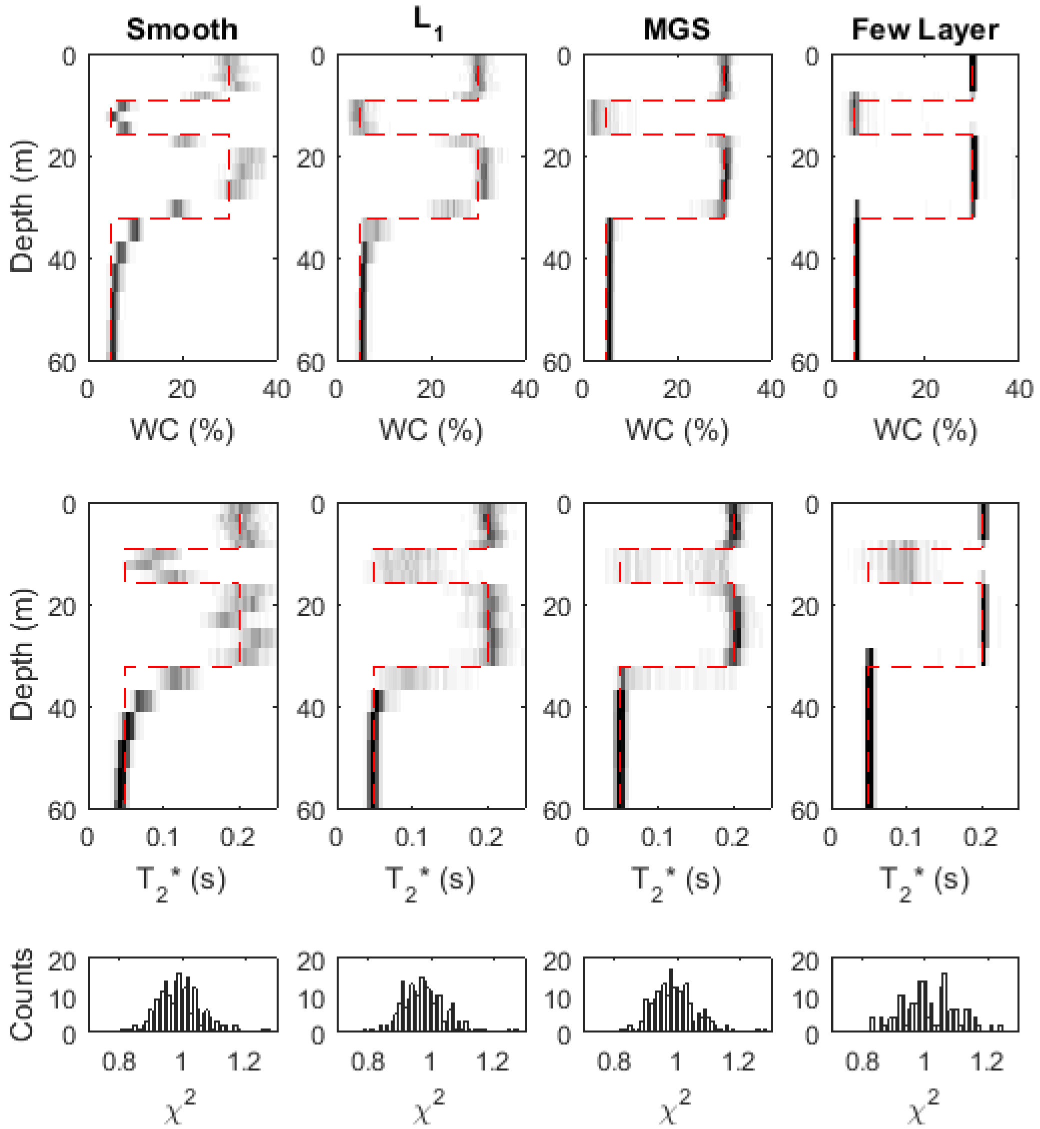

Figure 3. Histograms showing the water content (WC) (top row) and T_2* profiles (middle row) estimated from the inversion of 200 independent noisy data sets. The bottom row illustrates a histogram of the χ^2 for all 200 inversions. The dashed red line shows the true model (a four layer system consisting of two aquifers). Dark and white colors indicate bins with many and no counts, respectively. Columns left to right show the results for a many layer inversion using a smoothness stabilizer, a many layer inversion using an L_1 stabilizer, a many layer inversion using a MGS stabilizer, and a few layer inversion with 3 layers. The noise level is 20 nV. Black and white bins have 70 and 0 counts, respectively.

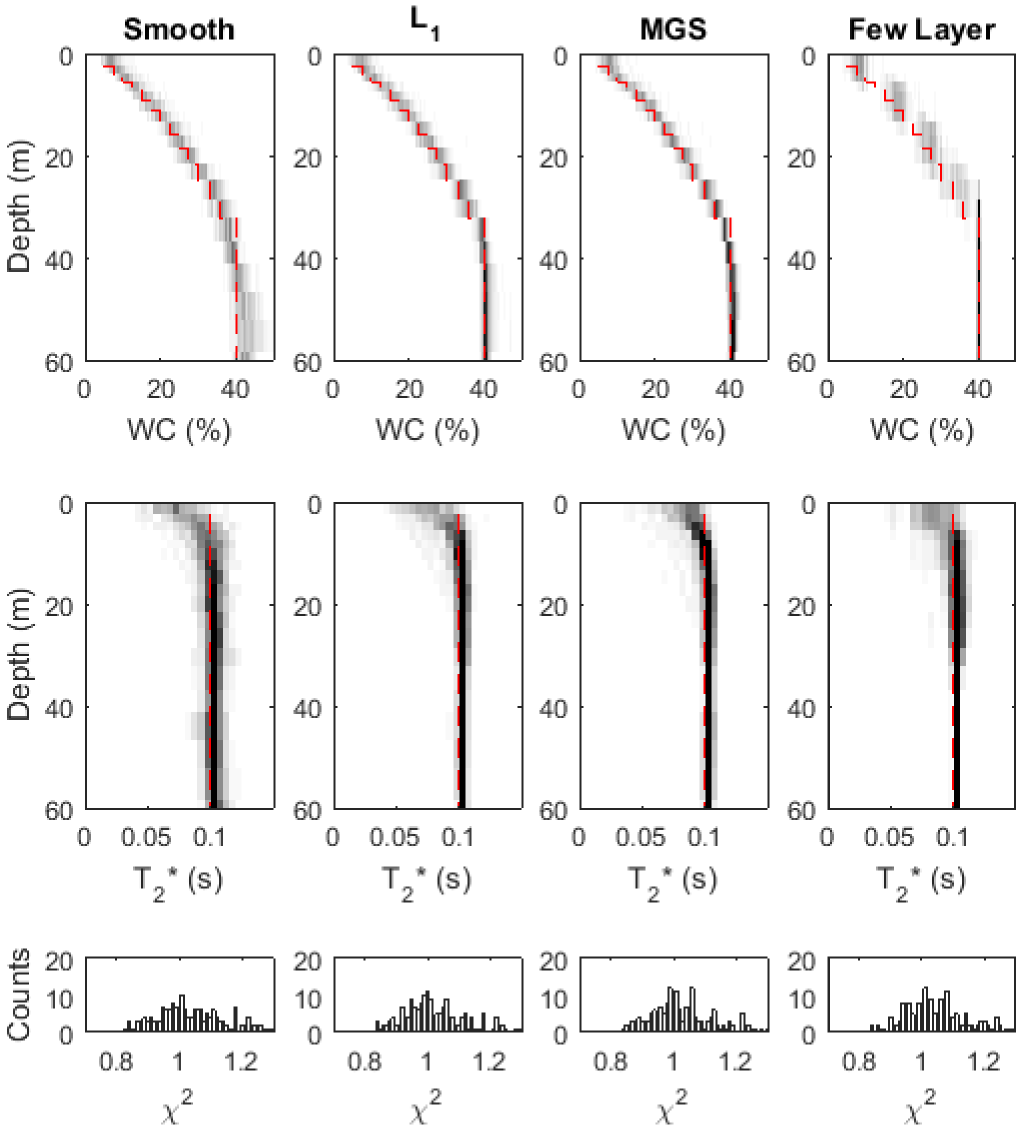

Figure 4. Histograms showing the water content (WC) (top row) and T_2* profiles (middle row) estimated from the inversion of 200 independent noisy data sets. The bottom row illustrates a histogram of the χ^2 for all 200 inversions. The dashed red line shows the true model (a smoothly increasing water content profile with a homogenous T_2*). Dark and white colors indicate bins with many and no counts, respectively. Columns left to right show the results for a many layer inversion using a smoothness stabilizer, a many layer inversion using an L_1 stabilizer, a many layer inversion using a MGS stabilizer, and a few layer inversion with 3 layers. The noise level is 20 nV. Black and white bins have 70 and 0 counts, respectively.

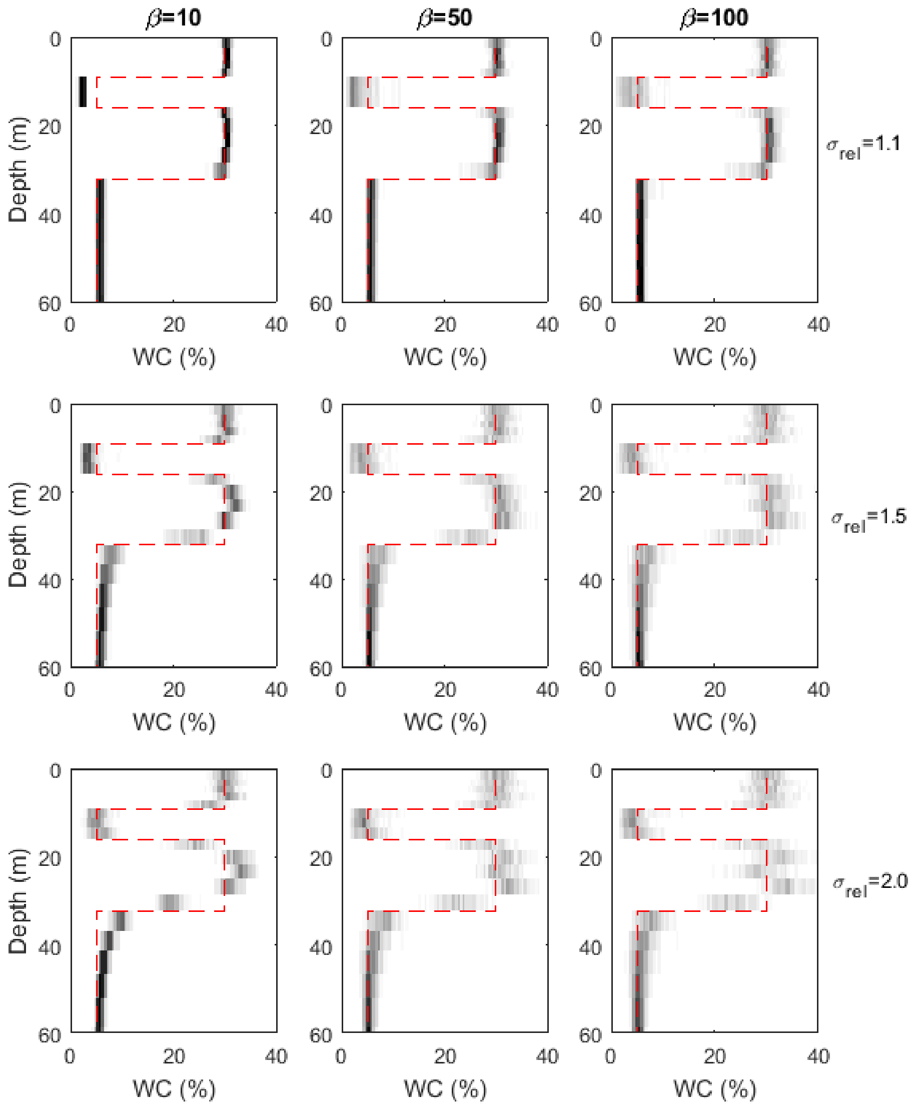

Figure 5. Histograms showing the influence of σ_{rel} and β on the estimated water content profile for the MGS stabilizer. The histograms are formed of the water content profiles resulting from the same 200 noisy data sets as in Figure 3. Each row and column correspond to a particular σ_{rel} and β, respectively. Dark and white colors indicate bins with many and no counts, respectively. The top left and bottom right represent the strongest and weakest regularization respectively. The noise level is 20 nV. Black and white bins have 70 and 0 counts, respectively.

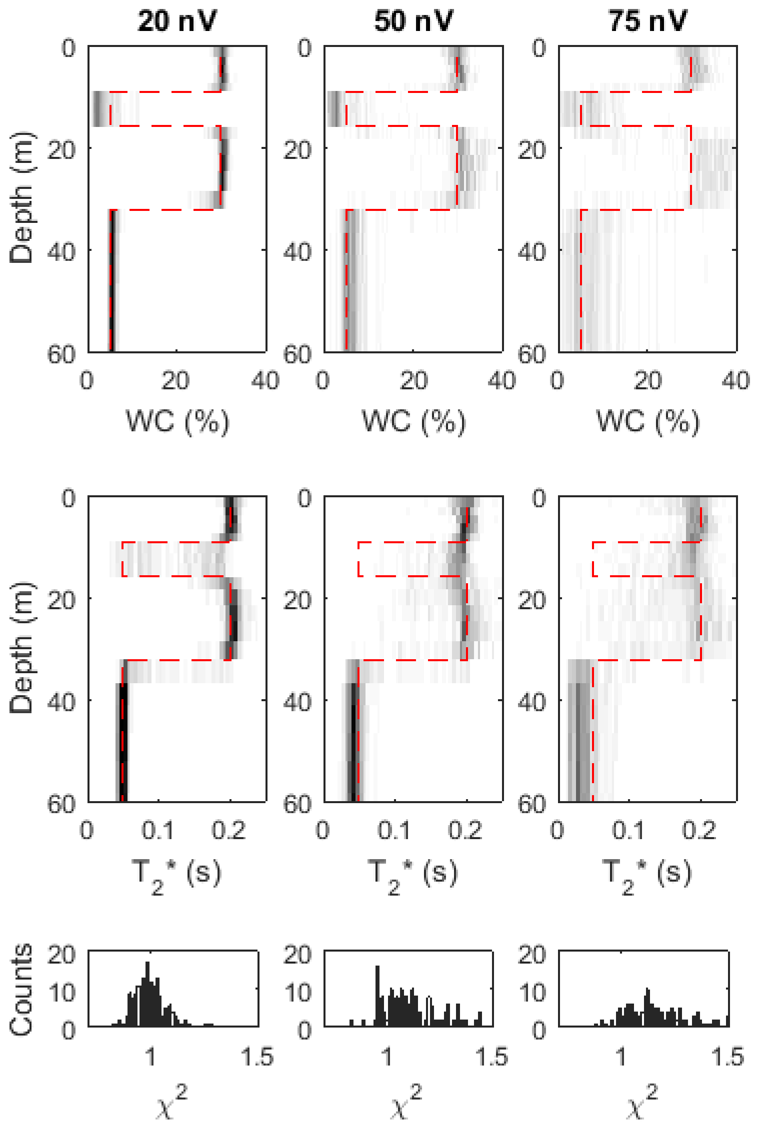

Figure 6. Histograms showing performance of the MGS stabilizer at varying noise levels. Each column corresponds to a particular noise level. The top and middle rows show histograms of the water content (WC) and T_2*, respectively, following the inversion of 200 noisy data sets. The bottom row illustrates a histogram of the χ^2 for all 200 inversions. The dashed red line shows the true model (same as in Figure 3). Dark and white colors indicate bins with many and no counts, respectively. Black and white bins have 70 and 0 counts, respectively.

Comparison of Stabilizer Functions for Surface NMR Inversions

Denys Grombacher[1], Gianluca Fiandaca[1], Ahmad A. Behroozmand[2], and Esben Auken[1]

[1]Department of Geoscience, Aarhus University, [2]Department of Geophysics, Stanford University

Corresponding author email : denys.grombacher@geo.au.dk

List of keywords : Surface nuclear magnetic resonance, groundwater, inversion

ABSTRACT

Surface nuclear magnetic resonance (NMR) is a geophysical technique providing non-invasive aquifer characterization. Two approaches are commonly used to invert surface NMR data: 1) inversions involving many depth layers of fixed thickness, and 2) few layer inversions without predetermined layer thicknesses. The advantage of the many layer approach is that it requires little a priori knowledge. However, the many layer inversion is extremely ill-posed and regularization must be used to produce a reliable result. For optimal performance the selected regularization scheme must reflect all available a priori information. The standard regularization scheme for many layer surface NMR inversions employs a L_2 smoothness stabilizer, which results in subsurface models with smoothly varying parameters. Such a stabilizer struggles to reproduce sharp contrasts in subsurface properties, like those present in a layered subsurface (a common near-surface hydrogeological environment). To investigate if alternative stabilizers can be used to improve the performance of the many layer inversion in layered environments the performance of the standard smoothness stabilizer is compared against two alternative stabilizers: 1) a stabilizer employing the L_1 norm and 2) a minimum gradient support stabilizer. Synthetic results are presented to compare the performance of the many layer inversion for the different stabilizer functions. The minimum gradient support stabilizer is observed to improve performance of the many layer inversion for a layered subsurface, being able to reproduce both smooth and sharp vertical variations of the model parameters. Implementation of the alternative stabilizers into existing surface NMR inversion software is straightforward and requires little modification to existing codes.

INTRODUCTION

Surface nuclear magnetic resonance (NMR) is a non-invasive geophysical technique providing insight into aquifer properties. The measurement involves pulsing strong oscillatory currents in a surface coil in order to generate a measureable NMR signal at depth that originates from the immersion of hydrogen nuclei in the Earth's magnetic field (Schirov et al., 1991; Hertrich, 2008). To gain insight into the spatial variability of aquifer properties, the amplitude of the pulsed current is varied to manipulate the spatial origin of the measured signal. This procedure is typically referred to as a sounding, where weak and strong currents produce signals from shallow and greater depths, respectively. The end product is a data set containing ~~various~~ NMR signals of differing spatial origins (although many signals have overlapping spatial origins). An inversion framework is used to estimate the underlying spatial distribution of aquifer properties consistent with the observed data. This involves minimizing an objective function that is used to penalize undesirable model characteristics, such as penalizing models that do not closely reproduce the observed data.

Several inversion schemes are commonly employed in surface NMR, such as the time step inversion (Legchenko and Valla, 2002), the QT-inversion that inverts the entire data cube simultaneously (Müller-Petke and Yaramanci, 2010), joint-inversion schemes coupling NMR and time-domain electromagnetic (TEM) data (Behroozmand et al., 2012) or NMR and electrical resistivity (Günther et al., (2012) data, and frequency-domain inversions (Irons and Li, 2014). In each case, the inversion result is a model of the subsurface aquifer properties (such as depth profiles of the water content and relaxation times that describe the duration of the NMR signal). For the purposes of this discussion we group surface NMR inversions into two categories: 1) inversions that use model domains consisting of many depth layers of fixed depths and thickness (referred to as many layer inversions), and 2) inversions involving relatively small model domains with few depth layers, where the inversion determines the thickness of each layer (referred to as few layer inversions). Each of the previously mentioned surface NMR inversion schemes may be implemented using either a many layer or few layer model domain.

In many layer inversions the number of model parameters is generally quite large (when compared with few layer inversions) and a regularization term must be included in the objective function to stabilize the ill-posed inversion (Tikhonov and Arsenin, 1977). The model that minimizes the objective function thus balances satisfactory data fit with the magnitude of the regularization term, which is controlled by the stabilizer function and the characteristics of the model. For optimal results the selected stabilizer function should: 1) return small values for the regularization term when the model exhibits features consistent with a priori knowledge about the site, and 2) return large values for models with characteristics inconsistent with a priori information about the site. The standard stabilizer in surface NMR is the L_2 smoothness stabilizer, which penalizes the square of the variation between neighboring model parameters. For a 1D depth sounding (the standard surface NMR experiment), this results in models that vary smoothly with depth. A limitation of such an approach is that the inversion struggles to reproduce sharp variations in water contents and relaxation times that may be present at the interface between lithologic layers of contrasting properties. To address this concern, an alternative stabilizer may be employed, such as the minimum support (Last and Kubik, 1983), minimum gradient support (Portniaguine and Zhdanov, 1999), or stabilizers based on L_1 norms (e.g. Ellis and Oldenburg, 1994; Loke et al., 2003). Mohnke and Yaramanci (2002) demonstrated the use of an L_1 stabilizer in surface NMR, but to our knowledge the smoothness stabilizer remains the standard in surface NMR.

For few layer inversions, a predetermined amount of layers is set and the inverted parameters are layer thicknesses, water contents, and relaxation times (Guillen and Legchenko, 2002; Mohnke and Yaramanci, 2002; Weichman et al., 2002). Due to the reduced number of model parameters (compared to the many layer inversion) no regularization term is included in the objective function. As a result, few layer inversions are well suited to produce models with sharp contrasts in water content and relaxation times between neighboring layers. An advantage of few layer inversions is that uncertainty in the estimated profiles can be readily quantified using Bayesian approaches such as Markov Chain Monte Carlo (Guillen and Legchenko, 2002; Weichman et al., 2002) or simulated annealing (Mohnke and Yaramanci, 2002). A limitation of few layer inversions is that they struggle to reproduce smoothly varying subsurface parameters and can exhibit strong sensitivity to the initial starting model (i.e. the a priori specification of the number of layers and layer properties).

In practice selection of a many layer versus few layer inversion scheme in surface NMR typically depends on how much a priori information is available. Many layer inversions are preferable given no a priori information, while few layer inversions may be preferable if a known number of layers are present. Few layer inversions are also commonly used if a well stratified subsurface is expected, given that many layer inversions typically result in models with smoothly varying subsurface parameters. However, this is not a result of the many layer inversion scheme directly, but rather a consequence that it generally employs a smoothness stabilizer. To balance the advantages of both inversion strategies for layered subsurfaces (i.e. the ability to reproduce sharp variations in model parameters without requiring extensive a priori information) the performance of several stabilizer functions is compared against the smoothness stabilizer; a minimum gradient support (MGS) stabilizer and a stabilizer employing an L_1 norm are investigated. Selecting alternative stabilizers does not require significant changes to existing inversions schemes. In this study, the inversion is performed using an iteratively reweighted least squares approach (Farquharson and Oldenburg, 1998), where a Taylor expansion of the objective function is used to form the model update. Within this framework alternative stabilizer functions are implemented by reweighting the roughness matrix within an L_2 norm (Vignoli et al., 2015; Fiandaca et al., 2015).

The MGS stabilizer (also referred to as focused or sharp inversion) provides the benefits of the many layer inversion but while maintaining the ability to produce models with sharp contrasts in properties (Portniaguine and Zhdanov, 1999). Briefly, the minimum gradient support stabilizer penalizes the number of sharp contrasts in the model regardless of their magnitude allowing the production of models with sharp interfaces between layers of relatively homogenous properties. The MGS stabilizer has been demonstrated to improve image sharpness for many layer inversion schemes in magnetic

(Portniaguine and Zhdanov, 1999), gravity (Portniaguine and Zhdanov, 1999), TEM (Vignoli et al., 2015), ERT (Pagliara and Vignoli, 2006), magentoteullurics (Zhdanov and Tolstaya, 2004), seismic (Zhdanov et al., 2006) and IP (Blaschek et al., 2008) studies. An additional stabilizer, employing an L_1 norm (instead of the L_2 norm present in the smoothness stabilizer) is also investigated. The L_1 norm penalizes the absolute value of the variation in model parameters. This allows for sharper contrasts in model parameters compared to the smoothness stabilizer (Loke et al., 2003), but not as readily as the MGS stabilizer. Mohnke and Yaramanci (2002) found that surface NMR inversions that use an L_1 stabilizer are better suited to producing models with sharp contrasts compared to the smoothness stabilizer. The L_1 norm is included in this comparison to compare its performance with the MGS stabilizer because of its ease of use. Synthetic results are presented to investigate the performance of each stabilizer for surface NMR inversion in the presence of a layered subsurface. Results of the many layer inversions are also compared against a few layer inversion. Discussion about the implementation of alternative stabilizers into existing inversion packages and guidelines for the use of the MGS stabilizer are also given.

BACKGROUND

The Surface NMR Inverse Problem

The standard measurement in surface NMR is the free induction decay, which involves measurement of the NMR signal following a single current pulse. To investigate the spatial variability of aquifer properties, the amplitude of the current pulse is altered to manipulate the spatial origin of the measured signal. The forward model is given by

$$\mathbf{d} = g(\mathbf{m}) + \mathbf{e}, \quad (1)$$

where **d** is a vector containing the measured NMR decays (for all current amplitudes for all time samples), and **m** is a vector containing the model parameters (water contents and T_2* in each depth layer). For a many layer inversion the number of depth layers, and their thicknesses are predetermined. For a few layer inversion the model **m** also contains the layer thicknesses. The g function describes the physics of the forward problem; it contains: 1) information about the expected spatial origin of the measured signal corresponding to the excitation pulse type, current amplitude, and pulse duration, 2) a spatial weighting based on the receiver sensitivity at each location in the subsurface, 3) the impact of a conductive subsurface on depth penetration and signal phase, and 4) a scaling parameter to estimate the magnitude of the equilibrium magnetization given the local magnetic field strength (local Earth's field strength) and aquifer temperature. **e** is a vector of the noise present in the data. Detailed derivation of the surface NMR forward model is given in Weichman et al. (2000).

To estimate the spatial distribution of aquifer properties an inversion is used to predict the model that balances satisfactory data fit with the magnitude of the regularization term. To determine this model an objective function $\Phi(\mathbf{m})$, described by

$$\Phi(\mathbf{m}) = \phi_d(\mathbf{m}) + \phi_s(\mathbf{m}), \quad (2)$$

is minimized. The $\phi_d(\mathbf{m})$ term describes the L_2 norm misfit between the predicted data ($g(\mathbf{m})$) and the observed data (normalized by the data uncertainty), while ϕ_s ($\mathbf{m}$) is the stabilizer function that determines the magnitude of the regularization term for the current model **m**. The $\phi_d(\mathbf{m})$ term is given by

$$\phi_d(\mathbf{m}) = \|\mathbf{Q}_d(\mathbf{d} - g(\mathbf{m}))\|_{L_2}^2, \quad (3)$$

where $\mathbf{Q}_\mathrm{d}^\mathrm{T}\mathbf{Q}_\mathrm{d} = \mathbf{C}_\mathrm{d}^{-1}$, i.e. the inverse of the data covariance matrix. The stabilizer function is described by

$$\phi_s(\mathbf{m}) = \left\|\mathbf{Q}_{\boldsymbol{R}}\,\mathbf{Rm}.\ \right\|_\eta^2, with\ \eta = L_2\ or\ L_1\ or\ MGS, \quad (4a)$$

and is necessary to stabilize the ill-posed inversion by penalizing models that exhibit undesired traits. $\mathbf{Q}_\mathrm{R}$ is a matrix used to weight the relative importance of the stabilizer function for each model constraint; $\mathbf{Q}_\mathrm{R}^\mathrm{T}\mathbf{Q}_\mathrm{R} = \mathbf{C}_\mathrm{R}^{-1}$, where $\mathbf{C}_\mathrm{R}$ is a matrix containing the variances of the constraints. The **R** matrix is called the roughness matrix, and is used to calculate the first order difference between the model parameters in neighboring depth layers. The η parameter corresponds to the norm used by the stabilizer (L_2 or L_1 or MGS). In this study the different norms are implemented using a reweighting matrix **W**(**m**) and an L_2 norm, where the stabilizer function is given by

$$\phi_s(\mathbf{m}) = \left\| \boldsymbol{Q}_R\, \mathbf{W}(\mathbf{m})\mathbf{Rm}. \right\|_{L_2}^2 . (4b)$$

The form of **W**(**m**) corresponds to the specific norm desired and can be determined by equating equation 4b with the equations describing the stabilizers in the following section. Equation 4b indicates that selection of a norm different than L_2 (the smoothness case) does not require significant modifications to existing inversion codes, it only requires the inclusion of an additional weighting matrix within the stabilizer.

To find the model **m** that minimizes equation 2 an iteratively reweighted least squares approach is used (Farquharson and Oldenburg, 1998), where the Taylor expansion of the objective function is used to determine the model update. This involves updating the estimated model iteratively; ultimately converging on a model that minimizes the objective function. Details about the inversion scheme employed in this manuscript are given in Auken et al., (2004), Vignoli et al. (2015), and Fiandaca et al. (2015). Note that the objective function (equation 2) does not contain a trade-off parameter that can be used to weight the relative importance of the ϕ_d and ϕ_s terms (the trade-off parameter is typically denoted by λ). The inversion scheme used in this study weights these terms equally, where the importance of the stabilizer term is controlled through the $\mathbf{Q}_R$ matrix that weights the relative importance of the stabilizer for each model parameter.

Selecting a stabilizer function

The stabilizer function stabilizes the inversion and allows the production of models with a desired property. This is done by penalizing models that exhibit an undesired trait. Equations 5a, 5b, and 5c illustrate the equations for a smoothness (L_2) stabilizer (the standard stabilizer in surface NMR inversions), the L_1 stabilizer, and the minimum-gradient support stabilizer, respectively:

$$\phi_s(\mathbf{m}) = \sum_k \left(\frac{(\Delta \mathrm{m})_k}{\sigma_k}\right)^2. \quad (5a)$$

$$\phi_s(\mathbf{m}) = \sum_k \sqrt{\left(\frac{(\Delta \mathrm{m})_k}{\sigma_k}\right)^2}. \quad (5b)$$

$$\phi_s(\mathbf{m}) = \frac{1}{\beta} \sum_k \frac{\left(\frac{(\Delta \mathrm{m})_k}{\sigma_k}\right)^2}{\left(\frac{(\Delta \mathrm{m})_k}{\sigma_k}\right)^2 + 1}, \quad (5c)$$

The $(\Delta\mathrm{m})_k$ term corresponds to the first order difference of the constrained parameters for the k^{th} constraint; i.e. $(\Delta\mathrm{m})_k = \mathrm{m}_{j(k)} - \mathrm{m}_{i(k)}$, where j(k) and i(k) represent the indices in the model vector of the parameters linked through the k^{th} constraint.~~;.~~ For the L_2 and L_1 stabilizers the σ_k term represents the strength of the constraint, because it controls the relative importance in the stabilizer function for the k^{th} constraint. Equation 5a indicates that the smoothness $\phi_s(\mathbf{m})$ increases proportional to square of the difference between neighboring model parameters. As such, sharp variations result in larger $\phi_s(\mathbf{m})$ and larger $\Phi(\mathbf{m})$. The minimization will therefore return smoothly varying models, as models with sharp transitions will be penalized. The L_1 stabilizer (Equation 5b) penalizes the absolute value of the difference in model parameters instead of the square of difference. As a result, smoothly varying models are still favored by the L_1 norm but sharp variations are penalized much less compared to the smoothness stabilizer. For both the L_2 and L_1 stabilizers , selection of σ_k controls the smoothness of the final model; large σ_k places little importance on the smoothness allowing more erratic profiles to be produced in order to further minimize $\phi_d(\mathbf{m})$, while small σ_k places more importance on model smoothness at the expense of a larger data misfit.

Formatted: Font: Not Bold

If a priori knowledge suggests sharp transitions are likely at a particular site, selection of a smoothness stabilizer is suboptimal given that it penalizes models with characteristics expected to be representative of the local hydrogeology. In this case, an alternative stabilizer may provide improved performance. For example, the minimum gradient support stabilizer (Portniaguine and Zhdanov, 1999) presents a more efficient implementation of ~~the~~ a priori knowledge of blocky structures. In this case, $\phi_s(\mathbf{m})$ is given by equation 5c; the form of the MGS stabilizer in equation 5c is chosen to be consistent with Vignoli et al., 2015. This form of the MGS stabilizer presents a parameterization allowing a simple understanding of the physical meaning of β and σ_k. Consider the effect of the MGS stabilizer in three regimes. In the $\left(\frac{(\Delta \mathrm{m})_k}{\sigma_k}\right)^2 \gg 1$ limit, which describes the sharp change in model parameters at the interface between layers of contrasting properties, the contribution to $\phi_s(\mathbf{m})$ approaches $1/\beta$. Therefore, the presence of a sharp transition in the model parameters is not penalized based on the magnitude of the model variation (as in the smoothness case) but rather penalized a fixed amount. In the $\left(\frac{(\Delta \mathrm{m})_k}{\sigma_k}\right)^2 \approx 1$ regime the contribution to $\phi_s(\mathbf{m})$ scales approximately with the square of the difference in model parameters. In the $\left(\frac{(\Delta \mathrm{m})_k}{\sigma_k}\right)^2 \ll 1$ regime there is little penalization and the contribution to $\phi_s(\mathbf{m})$ is small. This indicates that the MGS stabilizer will not severely penalize models containing sharp transitions, but will search for models with as few sharp transitions as possible with relatively homogenous properties between these sharp transitions (Portniaguine and Zhdanov, 1999). σ_k and β effectively control the extent of homogeneity within a layer, and the number of sharp transitions present in the final model, respectively. The value of β does not directly control to the number of sharp transitions present in the estimated model, but its magnitude does influence the number of transitions present. Models corresponding to large values of β have more transitions than models with small β.

Implementation of each norm in this study is done using the weighting matrix $\mathbf{W}(\mathbf{m})$, determined by equating equation 4b with equation 5a, 5b, or 5c. Note that for the L_1 and MGS stabilizers

W(**m**) depends on the current model, requiring that **W**(**m**) be recalculated every iteration. The computational cost of updating **W**(**m**) is not significant and each inversion proceeds at similar speeds in the case of a 1D surface NMR sounding. The stabilizer can also take other forms to describe different a priori conditions. In this manuscript the L_1 and MGS stabilizers are selected based on their less severe penalization of models containing sharp transitions in model parameters compared to the smoothness stabilizer.

RESULTS

Three synthetic surveys are presented to compare the utility of the L_1 and MGS stabilizers against the smoothness stabilizer for many layer surface NMR inversions. Each stabilizer is also compared against the results of a few layer inversion. Forward modelling and inversion of the synthetic data is performed using the AarhusInv software package (Auken et al., 2015), following the ~~Berhoozmand~~ Behroozmand et al. (2012) forward implementation. The inversion is performed using the amplitudes of the NMR signals (i.e. the in and out of phase components of the data are not treated separately). The inversion also bounds the estimated water contents to fall between 0.1% and 100%, while the relaxation times are bound between 5ms and 1.5 s. In each case FID measurements are simulated using a coincident transmit/receive 100 m square loop, a 30 ms on-resonance excitation pulse and 16 pulse moments sampled on the interval from 0.7 As to 8.5 As. The selected pulse moments are chosen to span a range typical of surface NMR field experiments. The subsurface resistivity is 1000 Ωm in each case, and is fixed during the inversion. This is equivalent to the inversions having a priori knowledge of the exact subsurface resistivity structure; a simple resistive subsurface is chosen to focus the comparison on the ability to estimate the subsurface parameters common to all surface NMR inversions (water content and relaxation times). In practice it is common for non-joint NMR-TEM inversion schemes to treat the subsurface resistivity structure (estimated form a separate TEM or other electrical survey) as fixed during the inversion. The Larmor frequency is set to 2138

Hz. Each inversion begins with a starting model corresponding to a half space of 15% water content and T_2* of 150 ms. The data are binned into 12 time gates of logarithmically increasing width. The earliest and latest time gates are centered at 41 ms and 445 ms, respectively. Gaussian white noise is added to the time gated data. To account for the varying widths of the time gates, the noise added to each time gate is scaled by the square root of the ratio of the time gate's width compared to the width of the first time gate. The stated noise levels refer to the standard deviation of the Gaussian used to generate the noise in the first time gate (width of the first time gate is 7.1 ms). The subsurface is discretized into 25 depths of increasing thickness to a depth of 110 m. The shallowest layers have thicknesses of 1.5 m and increase to a thickness of ~10m (layer thicknesses increase roughly logarithmically). Below 110m the subsurface is treated as a halfspace. A model discretization consisting of 25 depth layers was chosen to balance the opportunity to capture smoothly varying parameters without dramatically over parameterizing the subsurface. Increasing the number of depth layers places more importance upon the regularization. Further discussion about the approach used to discretize the subsurface is given in Behroozmand et al. (2012). Note that the layer boundaries for the synthetic subsurface models occur at the same depths as layer interfaces in the model discretization. In practice the depth discretization is unlikely to coincide with the true layer boundaries, in this case it would cause either smearing between two layers, or an error in identifying exact depth of the interface.

Formatted: Font: +Body (Calibri), pt, English (U.S.)

Formatted: Font: +Body (Calibri), pt, English (U.S.)

Formatted: Font: +Body (Calibri), pt, English (U.S.)

In each example, 200 noisy data sets are produced by adding different noise realizations to the same noise free data set. For the first three examples the noise level is 20 nV (i.e. the standard deviation of the Gaussian used to randomly generate noise for the first time gate is 20 nV). Although the signal to noise ratio (SNR) in each case depends on the subsurface model, this level of noise produces an SNR of ~50-80 for the three examples. For each noisy data set a water content and T_2* profile is estimated using a many layer inversion with a smoothness stabilizer, a many layer inversion with an L_1 stabilizer, a many layer inversion with an MGS stabilizer, and a few layer inversion. The 200 estimated water content and T_2* profiles produced by each inversion scheme are used to form histograms of the water content and T_2* values in each depth layer. The top two rows of Figure 1 illustrate several examples of how the histograms will be illustrated. The y-axes correspond to depth, the x-axes to either water content or T_2*, and the color scale indicates the number of counts present in each bin (black indicates a high number of counts and white indicates no counts). The water content and T_2* bins are 0.5% and 5 ms wide, respectively. The histograms allow the uncertainty of the resulting profiles to be estimated by examining the distribution of water contents and T_2* values within each depth layer. Low and high uncertainty correspond to depth layers with narrow black distributions and wide light grey distributions, respectively. Note that the histograms do not illustrate the full range of equivalent solutions as each inversion begins with the same starting model. However, the histograms remain a useful tool to provide insight into the uncertainty in the estimated profiles. For each stabilizer the results for single regularization strength are shown. The strength of the regularization is selected to produce the smoothest model that fits the data within error. The constraint strengths σ_k used in this study are relative to the magnitude of the model parameter $m_{i(k)}$; i.e. the constraint strength is effectively controlled by a parameter denoted σ_{rel}, where σ_k=($\sigma_{rel}m_{i(k)}$- $m_{i(k)}$). The inversion in this study is carried out in logarithmic model space, therefore $(\Delta \mathrm{m})_k$ becomes $log(\mathrm{m}_{j(k)}) - log(\mathrm{m}_{i(k)})$ and σ_k is estimated by subtracting the log-transformed parameter from the log-transformed upper limit of its confidence interval, i.e. σ_k becomes $log(\mathrm{m}_{i(k)} + \sigma_k) - log(\mathrm{m}_{i(k)})$. Therefore, the penalty $p = \frac{(\Delta \mathrm{m})_k}{\sigma_k}$ of equations 5a-c can be expressed in terms of σ_{rel} as $p = \frac{log(\mathrm{m}_{j(k)}) - log(\mathrm{m}_{i(k)})}{log(\mathrm{m}_{i(k)} - (\sigma_{rel}-1)\cdot \mathrm{m}_{i(k)}) - log(\mathrm{m}_{i(k)})} = \frac{log\left(\mathrm{m}_{j(k)}/\mathrm{m}_{i(k)}\right)}{log(\sigma_{rel})}$. ~~The constraint strengths σ_k used in this study are relative to the magnitude of the model parameter m_k; $\sigma_k = \sigma_{rel}\, m_k$ where σ_{rel} is a factor that defines the acceptable amount of variation~~. For example, σ_{rel}=1.1 means model parameter variations of ~10% is acceptable (i.e. should not be penalized severely). Given the noise level of 20 nV, σ_{rel}=1.5 was used for the smoothness and L_1 stabilizers, while for the MGS stabilizer σ_{rel}=1.1 and β=50. Note that for each stabilizer the water contents and T_2* parameters are given the same constraint strengths. Further discussion about the selection of the MGS stabilizer parameters is given in the discussion.

Figures 1, 3 and 4 contrast the performance of each stabilizer. The top row in each figure illustrates the estimated water content profiles, the middle row the estimated T_2* profiles, and the bottom row shows a histogram of the resulting ~~data residual norms (~~~~ϕ~~χ^2~~$_d$)~~ in each case. ~~Note that~~ χ^2~~ϕ_d~~ is unitless, as the data misfit (nV) is normalized by the data uncertainty (nV). χ^2~~ϕ_d~~ histograms clustered around 1 indicate good data fit (χ^2~~ϕ_d~~ is close to 1 because it is normalized by the number of data points). Columns one to three correspond to a many layer inversions that use a smoothness stabilizer, a L_1 stabilizer, and a MGS stabilizer, respectively. Column four illustrates the results of a few layer inversions that is given the correct number of layers. The true water content and T_2* profiles in each case are illustrated by the red dashed lines.

The first example (Figure 1) is a three layer system containing a single aquifer. The aquifer is 14 m thick (from 11-25 m depth) with a water content of 40% and T_2*=200 ms. The layers above and below this aquifer have reduced water content (5%) and faster T_2* (50 ms). The smoothness inversion (left column) accurately resolves the increased water content and T_2* layer producing reliable estimates of the water content and T_2* magnitudes in all three layers. The large contrast at the upper boundary is well-resolved by the smoothness stabilizer, while the lower boundary is smoothed over a larger depth range. The L_1 stabilizer (column 2) resolves the properties of all three layers well, capturing the sharp contrast at the upper layer boundary while also estimating a sharper transition to low water content and T_2* at the lower layer boundary compared to the smoothness stabilizer. The MGS stabilizer (column 3) produces similar results as the L_1 stabilizer and resolves both layer boundaries well. ~~The L_1 and MGS stabilizers overestimate the depth of the lower layer boundary to similar extents.~~ The estimated water contents and T_2* within the aquifer (layer 2) show less variation for the MGS case than the L_1 and smoothness stabilizer cases (darker narrower histograms). The few layer inversion, which was given the correct number of layers a priori, accurately reproduces the true model. ~~The lower boundary depth is slightly better resolved by the few layer inversion compared to the L_1 and MGS stabilizers.~~ In this example, the blocky true model is reproduced with high precision by the L_1, MGS, and few layer inversions, while the smoothness results make the identification the lower layer boundary more difficult. The bottom column of Figure 1 indicates that each inversion approach was able to fit the data to similar levels, with the data residual norms clustered around one. To give an example of the noisy data and quality of data fit Figure 2 illustrates the first of the two hundred noisy data sets (left panel) and the data residual (right panel) produced by the MGS stabilizer. The residual shows no structure (i.e. no large areas with consistent sign) and has a magnitude consistent with the noise level. The χ^2 ~~data norm~~ in this example is $\cancel{\phi_d =}$1.02. Figure 2B is representative of the residual produced by inversions resulting in similar magnitude χ^2 $\cancel{\phi_d}$.

The second example (Figure 3) is a slightly more complicated four layer system containing two aquifers. The two aquifers (layers 1 and 3) have water content of 30% and T_2*=200 ms. The layer separating these aquifers and the bottom layer have reduced water content (5%) and T_2* (50 ms). In this case, the smoothness inversion (left column) produces a smoothed version of the layered subsurface. The water content and T_2* are well estimated in each layer, but it is difficult to identify the layer boundaries given the smooth variations. For example, the upper and lower layer boundaries for layer 3 (the lower aquifer) are both spread over a 5-10m depth range. The L_1 inversion also reproduces the water content and T_2* magnitudes well, while better identifying the boundaries between the upper three layers. The MGS stabilizer produces similar results as the L_1 stabilizer, but with the lower boundary between layer 3 and 4 being more sharply resolved. The water content and T_2* values estimated within layers 1 and 3 are also more homogenous than the L_1 stabilizer (observed by narrower darker histograms for the MGS case compared to the L_1 case). Both the L_1 and MGS stabilizers struggle to resolve the magnitude of T_2* in the second layer. This is a consequence of the low water content at these depths which reduces the ability to resolve the magnitude of T_2*. For the few layer inversion, which is given the correct number of layers, the true model is well reproduced. The estimated T_2* value in layer 2 also has higher uncertainty (noted by the wide histogram). Overall, the few layer result is quite similar to that produced by the MGS stabilizer, with each layer boundary being well resolved. The L_1 and smoothness inversions are less able to capture the large contrast in properties at the lower boundary between layer 3 and 4. The bottom row of Figure 3 indicates that each inversion provides a similar level of data fit.

The third example (Figure 4) tests the performance of each stabilizer given a subsurface containing a smooth variation in water content. In this case the water content is 10% at the shallowest depth and increases roughly linearly to 40% at 37 m depth; T_2* is equal to 100 ms at all depths. Below 37m a homogenous 40% water content layer is present. The smoothness inversion (left column) accurately captures the slowly increasing water content profile, while estimating a smooth transition to lower water content at depth (below ~37 m). The L_1 stabilizer produces similar results as the smoothness case, capturing the smoothly increasing water content profile while better predicting a homogeneous water content below 37 m (narrow dark histograms). The MGS stabilizer also reproduces the true model well, with a similar prediction of the homogeneity below 37 m as the L_1 stabilizer. The T_2* profile is well resolved in all cases, except at the shallowest depths~~, where the lowest water contents are present~~. The systematic bias towards underestimated T_2* at the shallowest depths likely results from the T_2* at these depths having little impact on the overall data fit (given that these depths correspond to the lowest water contents). For the few layer inversion results, where the inversion is given 5 layers, a blocky stepwise increasing water content is predicted, with the overall structure in the water content being captured. The water contents at depths above ~37 m are more uncertain for the few layer inversion compared to the many layer inversions (wide light grey histograms). Below 37 m the few layer inversion accurately estimates the water content. The bottom row of Figure 4 indicates that each inversion scheme produces similar levels of data fit. For some noise realizations χ^2~~the data norm~~ is large (>~1.3) and the data fit is reduced. While increasing the number of layers for the few layer inversion will improves its ability to capture the smooth change in water content, the 5 layer model is shown given the preference for the model containing the fewest number of layers that provides satisfactory data fit.

Figures 1, 3, and 4 illustrate that the smoothness stabilizer is suboptimal when sharp layer boundaries are expected and the selection of an alternative stabilizer can improve the performance of the many layer inversion in the presence of a layered subsurface. Comparing the L_1 and MGS results indicates that the MGS stabilizer provides the best ability to reproduce a blocky subsurface structure when using a many layer inversion. Even in a smoothly varying subsurface, the MGS stabilizer produces a reliable result. The benefit of the MGS stabilizer is that it is able to resolve blocky structures without requiring knowledge of the number of layers a priori; the MGS results even provides similar performance to a few layer inversion given the correct number of layers. Note that for the depth discretization and noise levels used in these examples, a fixed level of regularization for the MGS stabilizer can be expected to provide flexible performance capable of resolving both smoothly varying and blocky subsurface structures. The few layer inversion also performs well for a layered subsurface provided that a sufficient number of layers is used in the inversion.

DISCUSSION

The selection of a many layer versus few layer inversion scheme should consider the available a priori information about the site. If little information about the subsurface is present, such as whether a layered or smoothly varying subsurface is present, the many layer inversion offers the benefits requiring no a priori specification about the number of layers. A preliminary many layer inversion can also be used to inform a subsequent few layer inversion, where the many layer result can be used to provide an initial model and helps in choosing the number of layers for the few layer inversion. Whether the result of the many layer inversion is to be used as the final estimated model or as a starting model for a few layer inversion it is beneficial to use a stabilizer well suited to producing models with features consistent with the expectations of the subsurface. Therefore, if a layered subsurface is expected the standard smoothness stabilizer is suboptimal. Both the L_1 and MGS stabilizer improve the ability of the many layer inversion to reproduce blocky structures. However, results produced by a many layer that uses an L_1 or MGS stabilizer are not necessarily more accurate than those produced by a smoothness stabilizer. Given equal levels of data fit, the results produced by each stabilizer represent equally-likely models. Similarly, few layer inversions providing similar data fits as the many layer inversion also provide equally-likely models. To decide between the potential models additional geologic information should be considered, such as the depositional environment which may help inform whether a layered or smoothly varying subsurface is more likely. The advantages of the L_1 and MGS stabilizer is that they provide a means for the many layer inversion to more readily produce sharp contrasts in properties.

Practical Considerations for using the MGS stabilizer in surface NMR

We now focus on the MGS stabilizer given that it provides the best ability to reproduce a layered subsurface when using a many layer inversion. The contribution of the MGS stabilizer to the objective function is controlled by two parameters, σ_k and β. In contrast, the smoothness and L_1 stabilizers are controlled by a single parameter σ_k. The additional parameter for the MGS stabilizer complicates the decision as to how the regularization strength should be selected. For the smoothness and L_1 cases the general rule for selection of the regularization strength is that the smoothest model producing satisfactory data fit should be selected, otherwise the inversion may introduce spurious features into the estimated profiles in an attempt to over fit the data. For the MGS stabilizer, selection of σ_k and β requires balancing the desired level of homogeneity within a layer with the number of sharp contrasts present in the estimated models. ~~In this study σ_k is relative to the model parameter m_k; i.e. the intralayer homogeneity is effectively controlled by a parameter denoted σ_{rel}, where $\sigma_k=\sigma_{rel}m_k$.~~ To illustrate the impact of each parameter on the performance of the MGS stabilizer Figure 5 shows the water content profiles for MGS inversions performed with different combinations of σ_{rel} and β given the same suite of 200 noisy data sets used to form Figure 3 (the two aquifer system). Each row and column corresponds to a particular σ_{rel} and β, respectively. The top middle panel is a reproduction of the MGS water content profiles from Figure 3. For small σ_{rel} (top row) the intralayer homogeneity is high, noted by dark narrow histograms. For larger σ_{rel} (rows 2 and 3), the intralayer homogeneity is reduced (wider light grey histograms) and the results begin to more closely resemble the smoothness water content profile in Figure 3. For increasing β (left column to right column) the likelihood of additional sharp contrasts is increased. In this example, this results in a blurring of the layer boundaries due to the reduced penalization of additional sharp contrasts in the final model. At this noise level (20 nV) each level of regularization fits the data to similar levels, except for the top left panel which produces a slightly poorer data fit. Given that the motivation to use an MGS stabilizer is to improve the ability of the many layer inversion to reproduce a layered subsurface, we recommend selecting a low σ_{rel} value (eg. fixing σ_{rel} to 1.1). This ensures that relatively homogeneous layers are produced, and effectively allows the regularization strength to be controlled by specifying a β value. The selected β should be as small as possible while still providing satisfactory data fit. For the depth discretization and noise levels used in these examples β=50 was observed to provide good performance. The corresponding T_2* profiles (for the same σ_{rel} and β pairs) exhibit similar trends (not shown~~ here~~).

Choosing the regularization strength also depends upon the signal to noise ratio. To investigate the performance of the MGS stabilizer for varying noise conditions Figure 6 illustrates the water content and T_2* profiles estimated using a many layer inversion with an MGS stabilizer for noise levels of ~~10,~~ 20, 50, and 75 nV. The true subsurface model in this example is the same as Figure 3. These noise levels roughly correspond to SNR of ~~~120,~~ ~60, ~25, and ~15, respectively. At the lowest noise condition~~s~~ (~~10 and~~ 20 nV) the true subsurface model is well reproduced, except for the T_2* value in layer 2~~. The T_2* magnitude in layer 2 is accurately resolved for a noise level of 10 nV, but becomes unresolved at higher noise levels~~. For noise levels of 50 and 75 nV, the estimated water content and T_2* profiles have larger uncertainty (wider light grey histograms) and no longer resolve the T_2* contrast between layer 2 and its neighbors. The data fit is also reduced at higher noise levels (as illustrated by the χ^2 histograms in the bottom row of Figure 6). In several cases with higher χ^2 ~~ϕ_d~~ the data residual plots show structure indicating a poor data fit. In these cases, the estimated profiles would be treated with high uncertainty. Note that the histograms effectively hide these poor profiles, as they are only 1 of 200 results. In practice, a high noise level may cause the MGS stabilizer to predict a sharp boundary at an incorrect depth or where no contrast exists at all. In this limit it may be preferable to use the MGS stabilizer to inform the number of depth layers present and to use this information as the a priori number of layers for a subsequent few layer inversion. The few layer inversion can then be used to readily quantify the uncertainty in the estimated profiles. Alternatively, in the high noise limit it may be preferable to use the smoothness inversion given that strong smoothness regularization may limit the introduction of spurious sharp contrasts (at the expense of resolving layer boundaries). At noise levels greater than that investigated in Figure 6 (which may happen depending on local noise conditions) the profiles show even greater uncertainty.

The σ_k and β parameters also depend on the depth discretization used in the many layer inversion. As such, we recommend that synthetic studies with similar models to those considered in Figures 1, 3, and 4 be performed using the same depth discretization that which will be used in the inversion of field data and with noise levels similar to the field data. This will help inform the range of σ_k and β parameters likely to provide satisfactory performance and will provide insight into how capable the inversion is of resolving a synthetic model with features similar to those present in the water content and T_2* profiles produced by the field data. Similar synthetic tests would also help select a regularization strength and understand the resolution of the final models for the smoothness and L_1 stabilizers.

CONCLUSIONS

The ability of the many layer surface NMR inversion to reproduce a layered subsurface is compared for several stabilizer functions. The standard stabilizer (smoothness stabilizer) penalizes sharp transitions in subsurface properties and is poorly suited to imaging layered subsurfaces. Two alternative stabilizers, an L_1

stabilizer and minimum-gradient support stabilizer, were found to improve the ability to identify sharp contrasts in layer properties. The minimum gradient support stabilizer is observed to greatly improve the ability of the many layer inversion to reproduce blocky structures. Although the L_1 norm is observed to also provide improved performance compared to the smoothness approach for layered subsurfaces, its improvement is less than the MGS stabilizer. Improving the utility of the many layer inversion in a layered environment benefits both the scenario where the model produced by the many layer inversion is used for building the conceptual model of the subsurface and the scenario where the many layer inversion is used to build an initial model and an estimate of the number of layers needed for a subsequent few layer inversion.

The form of the MGS stabilizer employed in this study provides a simple understanding of the role played by the two tunable parameters in the stabilizer function. The extent of water content and T_2* homogeneity within a layer for the MGS stabilizer is controlled by σ_k (we recommend that variations greater than 10% be penalized), while the number of sharp transitions present in the final model is influenced by β (small and large β lead to less and more transitions, respectively). Despite two tunable parameters, selection of appropriate inversion parameters is straightforward and a single set of parameters is observed to provide accurate results for a broad range of subsurface models. For the inversion of field data we recommend selecting inversion parameters based on observations from synthetic tests with simple models (like those present in Figures 1-~~3~~4), the same model discretization, and similar noise conditions as the field data. In high noise conditions it may be preferable to use the MGS many layer inversion to inform a few layer inversion, allowing the uncertainty of the estimated profiles to be more readily quantified. Alternatively, the standard smoothness stabilizer may be preferable to the MGS stabilizer in high noise environments in order to limit the introduction of spurious sharp contrasts that may be interpreted as layer boundaries. However, this comes at the expense of resolving sharp contrasts. In summary, the minimum gradient support stabilizer provides an effective means to improve the flexibility of the many layer surface NMR inversions.

ACKNOWLEDGEMENTS

Denys Grombacher was supported by funding from a Danish Council for Independent Research Postdoctoral Grant (DFF-5051-00002). Ahmad A. Behroozmand was partly supported by funding from the Danish Council for Independent Research.

REFERENCES

Auken, E. and Christiansen, A.V. 2004. Layered and laterally constrained 2D inversion of resistivity data. Geophysics, 69 (no. 3), 752-761.

Auken, E., Christiansen, A.V., Kirkegaard, C., Fiandaca, G., Schamper, C., Behroozmand, A.A., Binley, A., Nielsen, E., Effersø, F., Christensen, N.B., Sørensen, K., Foged, N., and Vignoli, G. 2015. An overview of a highly versatile forward and stable inverse algorithm for airborne, ground-based, and borehole electromagnetic and electric data. Exploration Geophysics 46 (no. 3), 223-235.

Behroozmand, A.A., Auken, E., Fiandaca, G. and Christiansen, A.V. 2012. Improvement in MRS parameter estimation by joint and laterally constrained inversion of MRS and TEM data. Geophysics 77 (no. 4), WB191-WB200.

Blaschek, R., Hordt, A. and Kemna, A. 2008. A new sensitivity-controlled focusing regularization scheme for the inversion of induced polarization data based on the minimum gradient support. Geophysics 73 (no. 2), F45-F54.

Ellis, R.G. and Oldenburg, D.W. 1994. Applied geophysical inversion. Geophysical Journal International 116, 5-11.

Farquharson, C.G. and Oldenburg, D.W. 1998. Non-linear inversion using general measures of data misfit and model structure. Geophysics 134, 213-217.

Fiandaca, G., Doetsch, J., Vignoli, G., and Auken, E. 2015. Generalized focusing of time-lapse changes with applications to direct current and time-domain induced polarization inversions. Geophysical Journal International 203 (no. 2), 1101-1112.

Guillen, A., and Legchenko, A. 2002. Inversion of surface nuclear magnetic resonance data by an adapted Monte Carlo method applied to water resource characterization. Journal of Applied Geophysics 50, 193-205.

Günther, T., and M. Müller-Petke, 2012. Hydraulic properites at the North Sea island of Borkum derived from joint inversion of magnetic resonance and electrical resistivity soundings. Hydrology and Earth System Sciences 16 (no. 9), 3279-3291.

Hertrich, M. 2008. Imaging of groundwater with nuclear magnetic resonance. Progress in Nuclear Magnetic Spectroscopy 53, 227-248.

Irons, T.P., and Li, Y. 2014. Pulse and Fourier transform surface nuclear magnetic resonance: comprehensive modeling and inversion incorporating complex data and static dephasing dynamics. Geophysical Journal International 199, 1372-1394.

Last, B.J., and Kubik, K. 1983. Compact gravity inversion. Geophysics 48 (no. 6), 713-721.

Legchenko, A., and Valla, P. 2002. A review of the basic principles for proton magnetic resonance sounding measurements. Journal of Applied Geophysics 50, 3-19.

Loke, M.H., Acworth, I. and Dahlin, T. 2003. A comparison of smooth and blocky inversion methods in 2D electrical imaging surveys. Exploration Geophysics 34, 182-187.

Mohnke, O., and Yaramanci, U. 2002. Smooth and block inversion of surface NMR amplitudes and decay times using simulated annealing. Journal of Applied Geophysics 50 (no. 1-2), 163-177.

Müller-Petke, M., and Yaramanci, U. 2010. QT inversion—Comprehensive use of the complete surface NMR data set. Geophysics 75 (no. 4), WA199-WA209.

Pagliara, G., and Vignoli, G. 2006. Focusing inversion techniques applied to electrical resistance tomography in an experimental tank. Proceedings of the 11th International Congress of the International Association for Mathematical Geology.

Portniaguine, O. and Zhdanov, M.S. 1999. Focusing geophysical inversion images. Geophysics 64 (no. 3), 874-887.

Schriov, M., Legchenko, A. and Creer, G. 1991. A new direct non-invasive groundwater detection technology for Australia. Exploration Geophysics 22 (no. 2), 333-338.

Tikhonov, A. N., and Arsenin, V. Y. 1977. Solutions of ill-posed problems. Washington, D.C., Winston.

Vignoli, G., Fiandaca, G., Christiansen, A.V., Kirkegaard, C. and Auken, E. 2015. Sharp spatially constrained inversion with applications to transient electromagnetic data. Geophysical Prosepcting 63, 243-255.

Weichman, P.B., Lavely, E.M. and Ritzwoller, M.H. 2000. Theory of surface nuclear magnetic resonance with applications to geophysical imaging problems. Physical Review E 62, 1290-1312.

Weichman, P.B., Lun, D.R., Ritzwoller, M.H. and Lavely, E.M. 2002. Study of surface nuclear magnetic resonance inverse problems. Journal of Applied Geophysics 50 (no. 1-2), 129-147.

Zhdanov, M., and Tolstaya, E. 2004. Minimum support nonlinear parameterization in the solution of a 3D magentotelluric inverse problem. Inverse Problems 20 (no. 3), 937-952.

Zhadnov, M.S., Vignoli, G. and Ueda, T. 2006. Sharp boundary inversion in crosswell travel-time tomography. Journal of Geophysics and Engineering 3 (no. 2), 122-134.

FIGURES AND FIGURE CAPTIONS

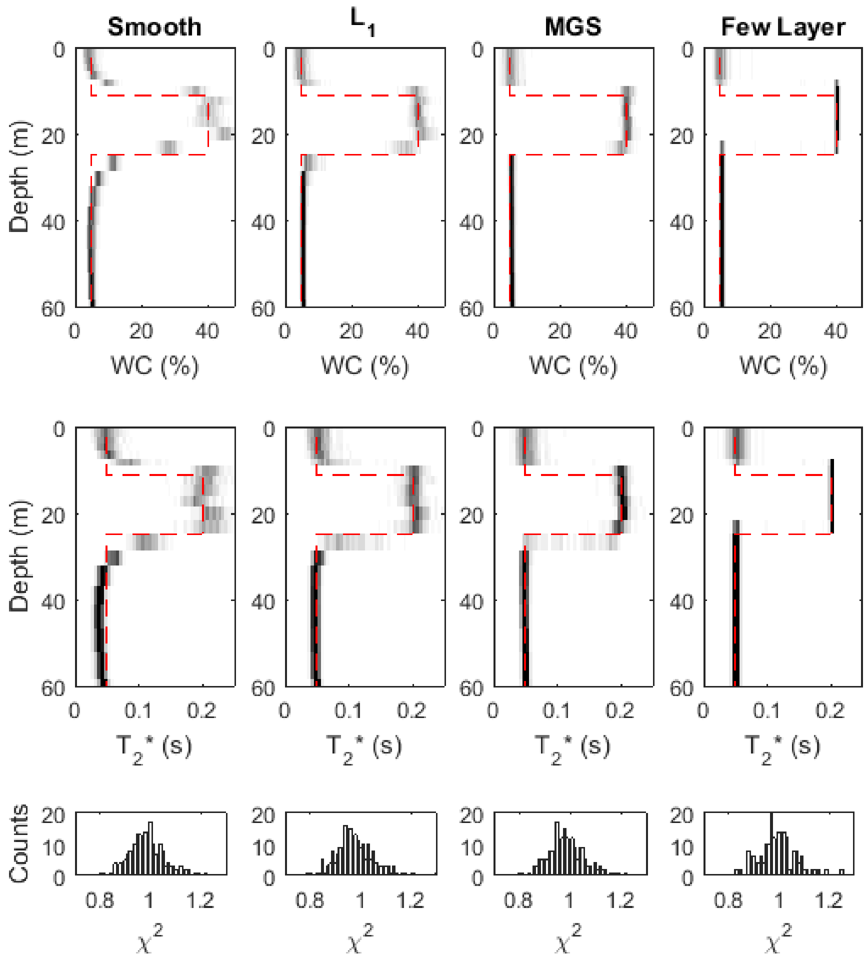

Figure 1. Histograms showing the water content (WC) (top row) and T_2* profiles (middle row) estimated from the inversion of 200 independent noisy data sets. The bottom row illustrates a histogram of the χ^2 ~~ϕ_d~~ for all 200 inversions. The dashed red line shows the true model (a three layer system with a single aquifer). Dark and white colors indicate bins with many and no counts, respectively. Columns left to right show the results for a many layer inversion using a smoothness stabilizer, a many layer inversion using an L_1 stabilizer, a many layer inversion using a MGS stabilizer, and a few layer inversion with 3 layers. The noise level is 20 nV. Black and white bins have 70 and 0 counts, respectively.

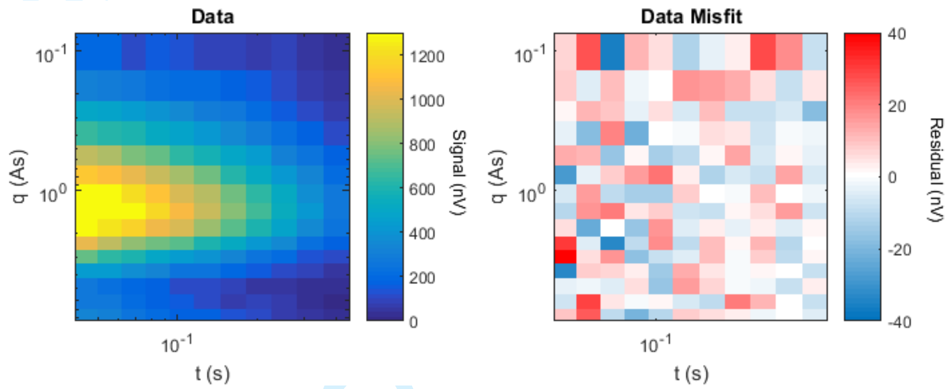

Figure 2. A) One of the 200 noisy data sets produced by the subsurface model in Figure 1. B) An example of the data residual produced by the many layer inversion using the MGS stabilizer. This data residual corresponds to a $\chi^2 \cancel{\phi_d}$ of 1.02 and is representative of that produced by other inversions with similar $\chi^2 \cancel{\phi_d}$.

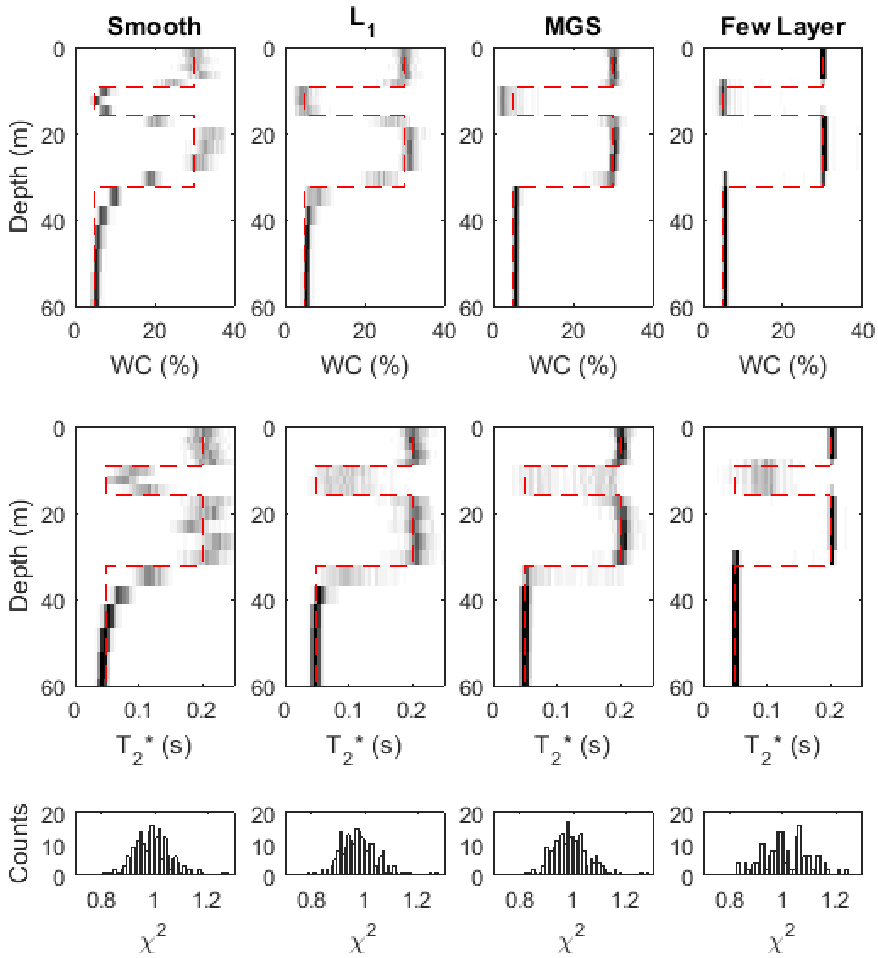

Figure 3. Histograms showing the water content (WC) (top row) and T_2* profiles (middle row) estimated from the inversion of 200 independent noisy data sets. The bottom row illustrates a histogram of the χ^2 ~~ϕ_d~~ for all 200 inversions. The dashed red line shows the true model (a four layer system consisting of two aquifers). Dark and white colors indicate bins with many and no counts, respectively. Columns left to right show the results for a many layer inversion using a smoothness stabilizer, a many layer inversion using an L_1 stabilizer, a many layer inversion using a MGS stabilizer, and a few layer inversion with 3 layers. The noise level is 20 nV. Black and white bins have 70 and 0 counts, respectively.

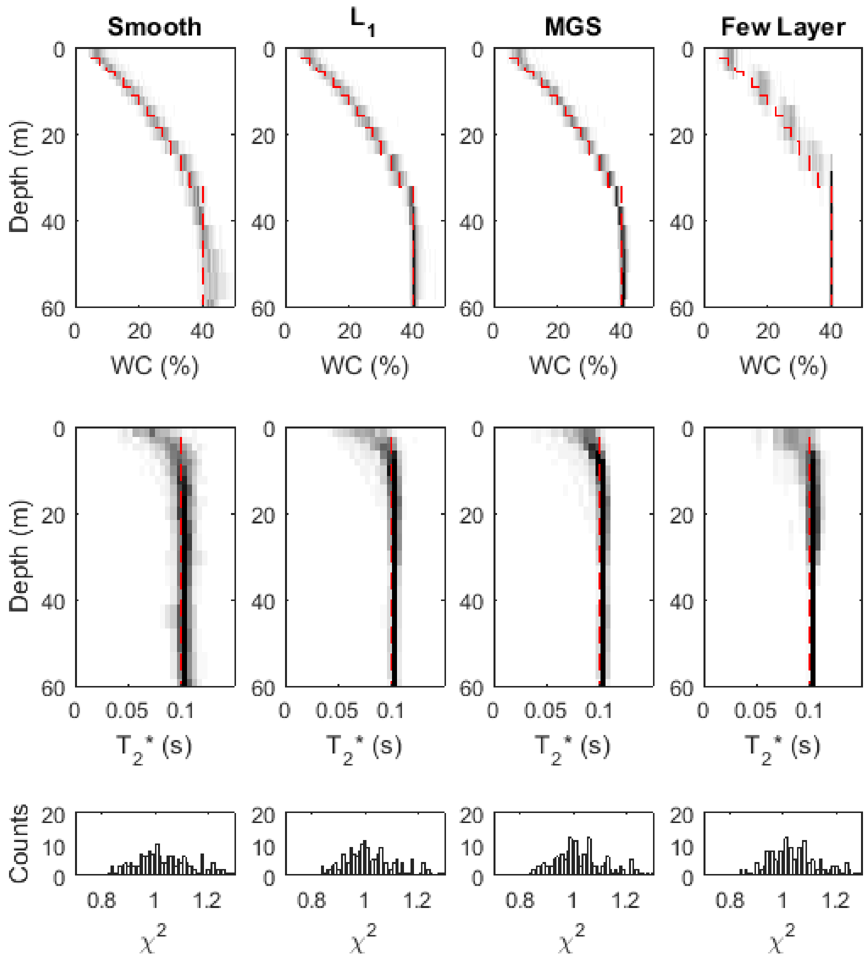

Figure 4. Histograms showing the water content (WC) (top row) and T_2* profiles (middle row) estimated from the inversion of 200 independent noisy data sets. The bottom row illustrates a histogram of the χ^2 ~~ϕ_d~~ for all 200 inversions. The dashed red line shows the true model (a smoothly increasing water content profile with a homogenous T_2*). Dark and white colors indicate bins with many and no counts, respectively. Columns left to right show the results for a many layer inversion using a smoothness stabilizer, a many layer inversion using an L_1 stabilizer, a many layer inversion using a MGS stabilizer, and a few layer inversion with 3 layers. The noise level is 20 nV. Black and white bins have 70 and 0 counts, respectively.

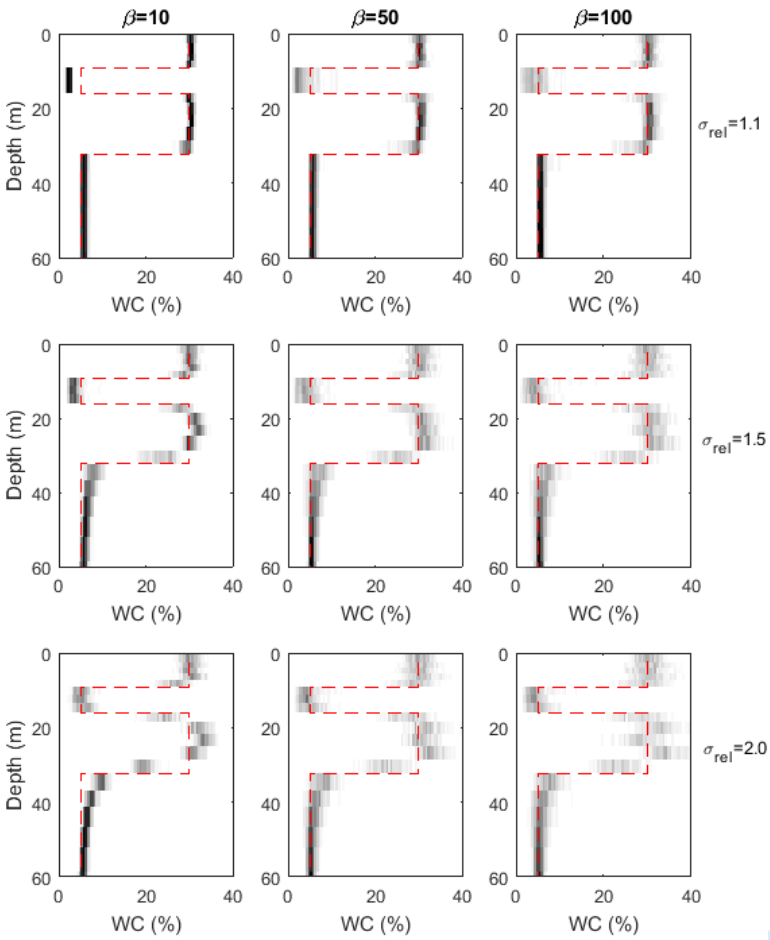

Figure 5. Histograms showing the influence of σ_{rel} and β on the estimated water content profile for the MGS stabilizer. The histograms are formed of the water content profiles resulting from the same 200 noisy data sets as in Figure 3. Each row and column correspond to a particular σ_{rel} and β, respectively. Dark and white colors indicate bins with many and no counts, respectively. The top left and bottom right represent the strongest and weakest regularization respectively. The noise level is 20 nV. Black and white bins have 70 and 0 counts, respectively.

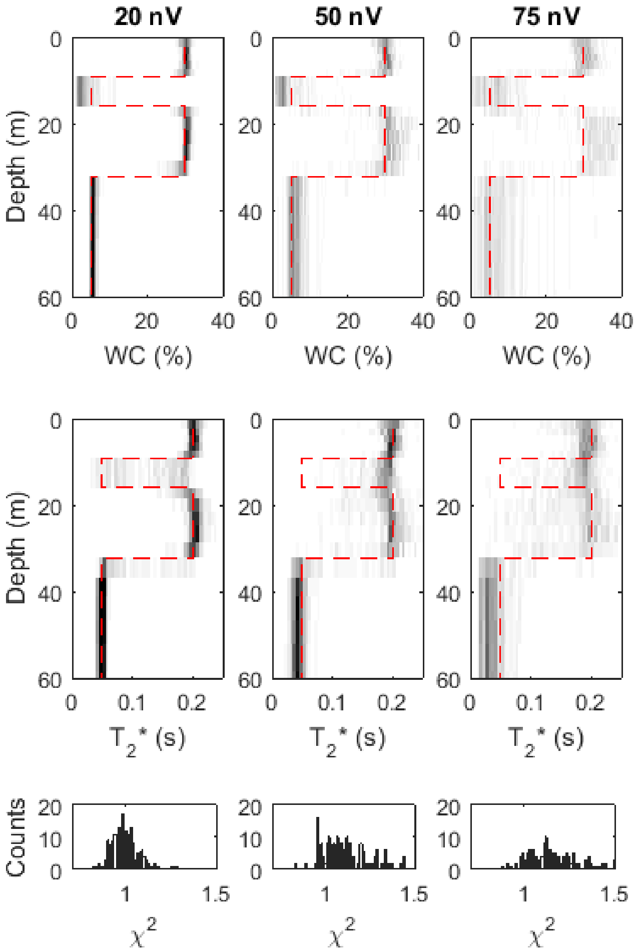

Figure 6. Histograms showing performance of the MGS stabilizer at varying noise levels. Each column corresponds to a particular noise level. The top and middle rows show histograms of the water content (WC) and T_2*, respectively, following the inversion of 200 noisy data sets. The bottom row illustrates a histogram of the ~~ϕ_d~~ χ^2 for all 200 inversions. The dashed red line shows the true model (same as in Figure 3). Dark and white colors indicate bins with many and no counts, respectively. Black and white bins have 70 and 0 counts, respectively.

EAGE Publications
Journal Submission Form (Green Open Access)

By signing this form the undersigned (hereinafter: **Author**) grants EAGE Publications B.V. (hereinafter: **Publisher**) the exclusive publication rights regarding author's publication specified below (hereinafter: the **Work**).

Note: this concerns Publisher's Green Open Access journal submission form. Other forms are available for Gold Open Access licenses and non-Open Access Works.

The Author

Name: Denys Grombacher
Address: P.P Ørumsgade 26, 4TH, Aarhus, Denmark, 8000
E-mail: denys.grombacher@geo.au.dk
Names of co-authors (if applicable): Gianluca Fiandaca, Ahmed A. Behroozmand, Esben Auken
Name and address of the owner of the Intellectual Property Rights (if applicable):

The Work

Title: Comparison of Stabilizer Function for Surface NMR Inversions

The Journal:

Name of the Journal: [to be filled in by EAGE]

Author declares the following

1. Publishing rights

1.1. Author hereby grants to Publisher the exclusive (also to the exclusion of Author) publishing rights in relation to the Work. To this effect, Author grants Publisher a worldwide exclusive perpetual and non-cancellable license to all Intellectual Property Rights regarding the Work.

1.2. The publishing rights as defined in clause 1.1. include – but are not limited to – the following:

(i) the right to make the Work available to the public in print or in digital format, including – but not limited to – the right to publish the Work in the Journal mentioned above and other journals of Publisher, and through any of its digital platforms including EarthDoc;

(ii) the right to promote, sell, distribute or otherwise (commercially) exploit the Work;

(iii) the right to make the Work fit for publication, including the right to amend the layout and title and to translate the Work in any language;

(iv) the right to duplicate the Work;

Initial Author: DG

(v) the right to grant (sub)licenses to third parties and to engage the services of third parties, explicitly including the companies within the group structure of Publisher;

(vi) the right to register the Work with collective rights organizations (such as the Copyright License Agency (UK), the Copyright Clearance Center (USA) and Stichting Pro/Stichting Reprorecht (the Netherlands);

(vii) any future and/or currently unknown means of exploitation of the Work by Publisher.

1.3. The term **Intellectual Property Rights** has the following meaning: all worldwide intellectual property and similar or related rights in the broadest sense of the term, or any entitlement thereto, especially those including – but not confined to – (1) copyrights, (2) portrait/image rights, (3) database rights, (4) design rights, (5) trademark rights, and (6) knowhow – including all powers related to these intellectual property rights, such as the exclusive rights to reproduce and make available to the public – and including any future Intellectual Property Rights, which is also deemed to refer to all entitlements which relevant national and international legislation accords or may accord to them.

1.4. The name of the Author and (if applicable) the name of the co-authors and/or owner of the Intellectual Property Rights as filled in above will be mentioned in the published Work, unless this cannot be reasonably be required.

1.5. This form constitutes a documented license [akte] as referred to in clause 2 under 3 of the Dutch copyright act [Auteurswet]. The Author shall cooperate at first request of EAGE and free of charge with the fulfilment of any legal formalities required for the grant of license.

2. Open Access rights

2.1. The Author has the right to make the Work available to the public after 12 months from the date of first publication of the Work by Publisher, under the condition that the Work contains a full reference to the source of the first publication by Publisher (i.e. the name, issue and year of publication of the Journal, the website of the Journal and the name of Publisher). The Author is not allowed to commercially exploit the Work, and therefore the Work can only be made available to the public free of charge. The Author is allowed to use the final text version of the Work, but is not allowed to use the lay-out made by Publisher, nor any graphics added by Publisher.

2.2. At first request of Publisher, the Author must provide evidence why the regulations regarding Open Access apply to the Work.

3. Delivery and acceptance

3.1. Author agrees to deliver to Publisher a complete draft of the Work. This includes the text of the Work in Word format and all other materials (such as images, data, tables, diagrams, graphics, maps or any other illustrative material) in electronic form. Any delivered materials should be in publishable (high resolution) format and comply with Publisher's guidelines as published on Publisher's website.

3.2. If the Work contains any materials (see examples in the previous clause) that are not created by Author or to which any third party can claim any Intellectual Property Rights or other rights, Author will provide Publisher with a written confirmation from such party that these materials may be used by Publisher and a royalty-free license is provided therefore.

3.3. If the Work contains quoted texts from other works these quotes need to comply with the copyright legislation applicable to quotes. At least the following conditions apply: the quoted work has already been lawfully published, only a reasonable portion of the original work is quoted, the persona rights of the original authors are respected, a proper reference to the original work is made in the foot notes, and the quote is used with a legitimate interest – for instance to discuss the quoted material or support the statements of the Author.

3.4. Publisher has the right to decide at its sole discretion not to publish the Work or to cease/withdraw the publication of the Work, in which case Publisher is not liable for any costs and/or damages resulting from this decision.

3.5. In case Publisher confirms that the Work will not be published in the Journal mentioned above, the license pursuant to article 1 will become non-exclusive. This means that the Author is allowed to publish the Work elsewhere.

4. <u>Royalty-free license</u>

The publication rights and license as defined in article 1 of this form concerns a royalty-free license, which means that Author is not entitled to any compensation. Author agrees with a royalty-free license because the Publisher gives the Author the opportunity to publish his Work in a renowned journal and the Publisher does not charge any costs for this publication, for instance for editing or adding (colour) pictures to the Work. Furthermore, the Work can be published by the Author as an Open Access Work.

5. <u>Warranties and indemnities</u>

5.1. Author undertakes and warrants that nothing prohibits the publication and exploitation of the Work pursuant to the license granted under article 1 of this form. More specifically, Author undertakes and warrants that:

(i) Author either owns, or is entitled to the use on the basis of a documented license, all Intellectual Property Rights or other rights pertaining to the Work and all materials included in the Work. In case the Author is entitled to use the Intellectual Property Rights on the basis of a license (for instance in case the employer is the owner), the Author will prove this (for instance by providing a copy of a written agreement, a written confirmation or a signature of approval under this form). In case of co-authors, article 7 of this form applies;

(ii) the Work has not been published before, nor that any license to publish the Work has been granted to any other party;

(iii) no rights of third parties, including but not limited to Intellectual Property Rights or any civil rights, will be infringed by the publication or exploitation of the Work;

(iv) the Work does not contain any libelous matter and the Work is not defamatory or obscene;

(v) the Work does not contain any faulty or illegal information or information that brings Publisher or other third party into disrepute.

5.2. Author shall fully indemnify Publisher and hold Publisher harmless for any costs and damages (direct or indirect) of Publisher in case of any non-compliance with the warranties mentioned in this article.

5.3. Author is fully responsible and liable for the contents of the Work. Publisher shall have no obligation to verify the contents of the Work or any other materials supplied by Author or to verify if publication thereof may cause any damages to (third) parties. The decision of Publisher to publish the Work or any other approval of the Work shall not be construed as an approval of the contents or confirmation of its legality.

6. Liability

6.1. To the fullest extent permitted by law, Publisher shall under no circumstances be liable for any indirect, consequential, special, exemplary, incidental or punitive damages, such as loss of (future) profits or other economic loss, damages for delay, third party claims and suchlike.

6.2. Publisher's total liability – including liability arising out of the publication of the Work, negligence, tort or warranty – shall be confined to the amount as paid out by the liability insurance of Publisher in the case concerned, and in case such damages are not insured or paid by the insurance company the total liability from Publisher towards Author shall be confined to an amount of € 50,000.00 (fifty thousand euros).

7. Infringement of Intellectual Property Rights

If the Intellectual Property Rights pertaining the Work are infringed, Publisher is granted the right to take such legal action as may be required to restrain such infringement or to seek damages and claim the profits made by the infringing party therefore. Such actions shall be taken at the sole discretion of Publisher and at its own cost and expense. Publisher is not obliged to take any legal action. Author herewith grants Publisher a power of attorney to take such legal measures. If Author wants to take legal actions on Author's own account, parties will discuss the approach of such matter.

8. Multiple authors

In case the Work is written by multiple authors as indicated by the Author of page 1 of this form, Author warrants that its co-authors agree with the publication and exploitation of the Work pursuant to article 1 and 2 of this form. Notwithstanding this warranty, Author will ensure that its co-authors will also sign this form.

Initial Author: DG

9. Miscellaneous

9.1. Publisher is allowed to assign its rights and obligations granted in this form to a third party, including a company within its group structure (for instance a mother, daughter or sister company). Author will – for as far as necessary – cooperate with such assignment.

9.2. This form shall be binding upon and inure to the benefit of the heirs, executors, administrators and assigns of Author, and upon and to the successors and assigns of Publisher.

9.3. This form is solely governed by and construed in accordance with the laws of the Netherlands. The application of the United Nations Convention on Contracts for the International Sales of Goods is precluded.

9.4. Any dispute arising between Author and Publisher pursuant or otherwise in relation to this form, which is deemed to include any that is regarded as such by either party, shall be resolved as much as possible through close consultation. In the event that parties are unable to resolve the dispute, it shall be adjudicated by a competent court of law in the city of Utrecht, the Netherlands, unless Publisher chooses to institute proceedings against Author before a competent court of law in Author's country of residence.

Thus agreed and signed by Author,

Date: Aarhus, Denmark
Place:
10/10/2016